European Commission

JRC SCIENCE AND POLICY REPORTS

Seismic Vulnerability of Chemical Racks in the Cross-Aisle Direction

Vincenzo Arcidiacono, Serkan Girgin, Elisabeth Krausmann

2014

Joint Research Centre

Report EUR 26953 EN

European Commission
Joint Research Centre
Institute for the Protection and Security of the Citizen

Contact information
Elisabeth Krausmann
Address: Joint Research Centre, Via E. Fermi 2749, 21027 Ispra (VA), Italy
E-mail: elisabeth.krausmann@jrc.ec.europa.eu

https://ec.europa.eu/jrc

JRC92620

EUR 26953 EN

ISBN 978-92-79-44410-4

ISSN 1831-9424

doi:10.2788/65727

Luxembourg: Publications Office of the European Union, 2014

Abstract

Information on the seismic response of chemical containers located in storage racks is very limited. Unfortunately, no clearly established data and statistics exist related to potential damage of chemical racking systems during earthquakes. Hence, this work presents an approach for developing fragility curves for chemical racking systems in the cross-aisle direction through dynamic non-linear analysis. It aims to simulate the structural behaviour of various racking systems in the cross-aisle direction for the worst-case scenario, in order to quantify the vulnerability of chemical racks in seismic areas and to better understand the associated natech risk. Analytical fragility curves and a fault tree model were derived and used to evaluate the probabilities of chemical containers falling from racks. The damage state limits were considered as four levels of intensity of loss of containment. Three damage modes (overturning, sliding, and buckling), 2 types of chemical containers (205 l metal drums and 1000 l IBCs), 3 types of rack base anchoring (unanchored, anchored-brittle, and anchored-plastic), and four rack heights (3, 4.5, 6, 7.5, 9 m) were considered in the analysis. Overall, 24 fragility curves were developed based on 26 strong motion records from the PEER Strong Motion database. However, the analytical method employed in this study can also be used for deriving fragility curves for other merchandise types of racking structures. In order to assess the natech risk of a chemical rack containing a flammable substance, to test the developed fragility curves, and to illustrate the natech risk assessment and mapping capabilities of RAPID-N, a case study based on the 1786 Olivieri earthquake scenario was conducted. The findings demonstrate that chemical racks loaded with IBCs are more vulnerable than those loaded with drums and although a very robust anchorage reduces the probability of collapse of the rack, it increases the probability of chemical containers falling.

Seismic vulnerability of chemical racks in the cross-aisle direction

Vincenzo Arcidiacono, Serkan Girgin, Elisabeth Krausmann

Abstract

Information on the seismic response of chemical containers located in storage racks is very limited. Unfortunately, no clearly established data and statistics exist related to potential damage of chemical racking systems during earthquakes. Hence, this work presents an approach for developing fragility curves for chemical racking systems in the cross-aisle direction through dynamic non-linear analysis. It aims to simulate the structural behaviour of various racking systems in the cross-aisle direction for the worst-case scenario, in order to quantify the vulnerability of chemical racks in seismic areas and to better understand the associated natech risk. Analytical fragility curves and a fault tree model were derived and used to evaluate the probabilities of chemical containers falling from racks. The damage state limits were considered as four levels of intensity of loss of containment. Three damage modes (overturning, sliding, and buckling), two types of chemical containers (205 l metal drums and 1000 l IBCs), three types of rack base anchoring (unanchored, anchored-brittle, and anchored-plastic), and four rack heights (3, 4.5, 6, 7.5, 9 m) were considered in the analysis. Overall, twenty-four fragility curves were developed based on twenty-six strong motion records from the PEER Strong Motion database. However, the analytical method employed in this study can also be used for deriving fragility curves for other merchandise types of racking structures.

In order to assess the natech risk of a chemical rack containing a flammable substance, to test the developed fragility curves, and to illustrate the natech risk assessment and mapping capabilities of RAPID-N, a case study based on the 1786 Olivieri earthquake scenario was conducted. The findings demonstrate that chemical racks loaded with IBCs are more vulnerable than those loaded with drums. Moreover, although a very robust anchorage reduces the probability of collapse of the rack, it increases the probability of chemical containers falling.

Table of Contents

1 Introduction

A number of hazards can be created when storing packaged dangerous substances. These hazards can affect people working within the storage site, the emergency services in the event of an accident, the general public off site and the environment. In a chemical warehouse (Figure 1), fire is generally considered to be the greatest hazard (HSE, 2009). In rare cases, certain stored substances can undergo violent decomposition when engulfed in flame, and result in an explosion. Either event can be trigged by natural hazards or disasters. These accidents are commonly referred to as natech accidents (Showalter & Myers, 1994; Krausmann et al., 2011).

For example, in the 1970 Tarnava flood, the chemical platform Tarnaveni was affected (Boca et al., 2010). Water entered the warehouse where 800 tons of carbide was stored in wooden barrels. The exothermic reaction caused a powerful explosion, which destroyed all buildings within a radius of 200 m around the warehouse. During the 1999 Kocaeli earthquake, a fire of limited size in a chemical warehouse was reported shortly after the earthquake (Girgin, 2011). Dangerous substances stored in glass containers fell down because of the strong ground motion and the contents were spread onto the ground, causing the fire. In 11 March 2011, some warehouses in Japan – because of the earthquake and the tsunami – suffered major releases of hazardous materials, because packed products fell from racks and were ripped open (Krausmann & Cruz, 2013).

During a natural event, safety in a chemical warehouse depends both on the structural performance of the building and on the dynamic performance of the storage racks and their contents (Castiglioni, 2008). In particular, earthquake ground motions can cause storage racks to collapse or overturn if they are not properly designed, installed, maintained, and loaded. In addition, individual packages or containers may spill or topple off, potentially causing releases of material.

Figure 1. Intermediate Bulk Containers stored in warehouse racking (HSE, 2009).

Information on the seismic response of chemical containers located in storage racks is very limited. Unfortunately, no clearly established data and statistics exist on potential damage of chemical racking systems during earthquakes. Frequently, after an earthquake event, loss of dangerous substances has been reported, with or without contemporary failure of the steel rack structural system (Castiglioni, 2008). Most probably, the structural failures were a consequence of the falling pallets and of the impact of the goods on the beams at the lower levels, creating a progressive dynamic collapse (Ng et al., 2009; Bajoria, 1986). Generally, failures of racks in earthquakes are most commonly reported in the cross-aisle direction (Castiglioni, 2008).

This study aims to simulate the structural behaviour of various racking systems in the cross-aisle direction for the worst-case scenario in order to quantify the vulnerability of chemical racks in seismic areas and to better understand the associated natech risk. A set of analytical fragility curves based on numerical simulation considering both structural parameters and the variation of motion intensity was developed. The damage state limits were considered as four levels of

intensity of loss of containment. A fault tree model was used to evaluate the overall loss probability of chemical racks with respect to the peak ground acceleration (*PGA*). A simple case study to assess the natech risk of chemical racks containing flammable substances based on the 1786 Olivieri's earthquake scenario was conducted using the JRC's RAPID-N tool for rapid natech risk assessment and mapping (Girgin and Krausmann, 2013).

The next section starts with a brief description of the typical seismic vulnerabilities of racking systems and a summary of the common layout and structural characteristics of chemical racks. Then, the proposed dynamic models used to describe the losses of dangerous substances, and the fault tree model are described. The numerical results, the case study, and the conclusions of the proposed methodology and presented fragility curves are treated in the last two sections of this report.

2 Vulnerability of Racking Systems

The rack industry calls the longitudinal direction of racking systems the down-aisle direction and the transverse direction, the cross-aisle direction. The cross-aisle frame dominates the dynamic behaviour in the cross-aisle direction of racking system when subjected to earthquake forces (Castiglioni, 2008). Despite their lightness, racking systems carry a very high live load (many times larger than the designed dead load) and can reach a considerable height. These systems – if installed in a seismic zone – are vulnerable to the dynamic forces generated by the earthquake motion. The most recent seismic design standards for steel storage racks set specific tests to evaluate the performance of the key components (R.M.I., 2002a; R.M.I., 2002b; FEM, 2001; RAL, 1990; A.S., 1993; FEM, 2005).

A convenient and widely adopted way to define the typical seismic vulnerability is the use of the seismic fragility concept. A seismic fragility curve is defined as the "conditional probability of an infrastructure type reaching or exceeding a specific level of damage" (Sasani et al., 2002). Empirical fragility curves are the most reliable, but due to the scarcity and ambiguities of damage observations, their derivation is not always possible. Therefore, in our case, analytical curves are the most appropriate, because it is possible to increase the observational data set by performing numerical analyses. These are evaluated from the statistical study of the numerical dynamic analysis results based often on simplified structural models (Calvi, 1999; Crowley et al., 2004).

The loss of dangerous substances during an earthquake can endanger the life of the employees as well as of the population near the chemical warehouse. These losses can occur with the collapse of the entire rack as well as the falling of its containers due to the sliding and/or overturning of pallets or of containers. The sliding or overturning of chemical containers, due to the action of peak floor acceleration on the racks, and their consequent fall represents a limit state that might occur during a seismic event also in the case of a well-designed storage rack. These phenomena depend only on the dynamic friction coefficient between the pallet and the steel beam of the rack, and on the geometry of the containers. Therefore, in determining the likelihood of losses for racking systems, it is possible to identify four damage modes that could be sources for overall system losses. These modes are:

1. o*verturning* of the racking system due to the rocking motion and the failure of the anchorage,
2. failure of the racking system due to the *buckling* of the bracing system,
3. falling of chemical containers from the rack due to the *sliding* motion, and
4. o*verturning* of the containers with the subsequent fall from the rack.

Their individual contributions can be combined with a *fault tree analysis* to evaluate the overall losses. The lognormal cumulative distribution was selected to model the seismic vulnerability of each of the above damage modes j, since it has been very frequently used for representing fragility relationships (FEMA, 1999; Pinto et al., 2004; Singhal & Kiremidjian, 1996). The probability for the j^{th} damage mode $P_j[DS|MI_{i,j}]$ to exceed a certain damage state, given a specific value of Motion Intensity at the rack's i^{th} floor ($MI_{i,j}$), depends hence on the two parameters μ_j and σ_j of the lognormal distribution. These parameters have to be inferred by fitting the results of the analytical models with a lognormal curve. For each damage phenomenon, the model corresponding to the best fitting with empirical data is assumed as fragility curve:

$$P_j\left[DS\middle|MI_{i,j}\right]=\Phi\left(\frac{\ln\left(MI_{i,j}\right)-\mu_j}{\sigma_j}\right) \quad (1)$$

where $MI_{i,j}$ is the motion intensity at the i^{th} rack floor for the j^{th} damage mode; and Φ is the lognormal cumulative distribution function.

There are a lot of studies in the literature that explain the structural properties of representative steel industrial storage racks (Blume, J. A. & Associates, 1973; Krawinkler et al., 1979; Chen et al., 1980a; 1980b; 1981). In these studies, the fundamental periods of vibration – measured over a range of actual merchandise loading conditions – ranged from 0.2-1.0 s in the cross-aisle direction and from 0.7-3.0 s in the down-aisle direction. The first mode damping ratios ranged from 0.5-3.0% in the cross-aisle direction and 3-9% in the down-aisle direction. An experimental study of Filiatrault and Wanitkorkul (2004) observed that the racking systems are significantly more flexible and ductile, and have more dissipative capacity, in the down-aisle direction than in the cross-aisle direction. Since we are interested in worst-case situations, this study focuses on the cross-aisle direction.

The standard chemical containers used in chemical warehouses (Figure 2) are individual packages stored on pallets for solid and powdery substances and 205-litre metal drums and Intermediate Bulk Containers (IBC; 450-3000 litre) for liquid substances. The quantity limits are regulated according to their class (i.e., the groupings, numbered from 1 to 9, into which dangerous goods are assigned on the basis of a common single or most significant hazard), packing group (i.e., one of three groups into which dangerous goods are divided for packaging purposes according to their degree of danger, and that are ranked in a decreasing order of danger: 1=high, 2=medium, and 3=low.), and physical state (ADR, 2012).

Figure 2. Standard chemical containers used in chemical warehouses (HSE, 2009).

Storage racks are normally configured as two rows of racks that are interconnected. Storage rack bays are typically 1.0-1.1 m deep and 1.8-2.7 m wide and can accommodate two or three pallets. The overall height of pallet rack structural frames found in retail warehouse stores varies between 5 and 6 m while in industrial warehouse facilities it ranges from 12 to 15 m or more (Castiglioni et al., 2008). Generally, the height for combustible storage is limited by general fire-protection and life safety requirements (OFC, 2006; HSE, 2009). For example, the Oregon Fire Code (OFC, 2006) limits the storage height to 9.1 m for high-hazard commodities. Storages with greater heights are classified as extra-high-rack combustible storage and require special fire protection provisions. The main factors that influence the stability of the racking installation are the height-to-depth ratio and whether it is fixed to the floor or other suitable parts of the building structure (HSE, 2007). The UK Health and Safety Executive (HSE) requires that freestanding racks (i.e., not fixed to the floor) should not be used in areas where lift trucks, order pickers or other mechanical handling devices are used. Otherwise, it requires that when the height/depth ratio does not exceed 6:1 all uprights adjacent to aisles and gangways have to be fastened down with bolts (to reduce the risk of damage from accidental impact). If the height/depth ratio is higher than 6:1 but does not exceed 10:1, all uprights have to be fastened down. In any case, it is

important to note that in this regulation the bolts are designed to withstand the lateral impact of a mechanical device.

Braced frames are typically used in the structural system in the cross-aisle direction. A recent study of Castiglioni et al. (2008) focuses on the seismic structural behaviour of steel selective pallet storage racks. In their study, typical structural elements in pallet storage racks were tested and characterized. Besides, friction coefficients (static μ_S and dynamic μ_d) between pallets and beams (i.e. wood or plastic vs. painted steel) were studied; the findings are used in the present study. The details of steel racking system dimensions, of mathematical structural models, and chosen seismic records are described in the following sections.

3 Model Development for Cross-aisle Frames and Containers

Typical natech consequence scenarios (explosion, fire, toxic dispersion) depend on the type and total amount of released dangerous substances and their storage conditions (Tugnoli et al., 2007). Many difficulties arise in the prediction of a rack's structural behaviour like buckling of the bracing or the failure of the anchoring, as it is affected by the particular geometry of their structural elements (Baldassino & Zandonini, 2001). Therefore, we split the dynamic failure of the cross-aisle frame and of chemical containers into three macro-models that consider the three different failure mechanisms, i.e., overturning, sliding, and buckling.

In this report, for reasons of simplicity, only pure sliding and pure rocking were investigated, neglecting the slide-rock mode (Shenton, 1996). Sometimes, the pallet can get stuck and thus it cannot slide. Since the worst case was investigated, it was assumed that the peak floor acceleration for the rocking motion is not affected by the sliding of the pallet. In case of liquid chemical substances, the sloshing motion was neglected considering that the containers were treated as rigid blocks. In order to simplify the models, the length of the rack in the downward direction in the corridor was considered to be infinite. This assumption is reasonable and should not affect the results, because generally the length of the structure is much greater than its depth.

In this study, the damage states (X_j<1=no fall; X_j≥1=fall) of chemical containers (i.e., local failures) and of the upright frame (i.e., global failure) were related to the vulnerability (i.e., damage state) of the racking system (Figure 3a) to losing its containment (i.e., when chemical containers are dropped from the frame). The damage states (*DS*) were defined with four levels of intensity of loss of rack containment (in other words, the percentage of containers that fall from the frame): *DS0*=no losses, *DS1*=moderate losses (≥30% of containers fall), *DS2*=extensive losses (≥60% containers fall), and *DS3*=complete loss of containment (100% containers fall). It is assumed that once the containers fall, the complete amount of substance contained therein will be released. As mentioned above, fault tree analysis was used to determine the likelihood of losses from racking systems due to the four damage modes introduced in Section 2 and discussed in more detail in the following sections. The fault tree model for earthquake-generated losses from chemical racks adopted in this study is presented in Figure 3b. The probability *P* of being in or exceeding a given *DS*, i.e. the vulnerability of a racking system to lose its containment, is analytically given by:

$$P\left[DS\middle|PGA\right]=\begin{cases}1 & \text{if } DS = DS0\\ \max\left\{\max\limits_{j=1,2}\left(P_j\left[X_j\geq 1\middle|MI_{0,j}\right]\right),\ \prod\limits_{k=0}^{n_{FF}(DS)-1}P_{L,k}\right\} & \text{otherwise}\end{cases} \quad (2)$$

where n_{FF} is the number of simultaneous floor failures – i.e., when all containers of a given floor fall – required to cause an amount of loss that is defined by a given *DS*; X_j are parameters that describe the failure of the system for the j^{th} damage mode (i.e., the system falls if X_j≥1); $MI_{0,j}$ is the motion intensity at the ground floor; $P_1[X_1\geq 1|MI_{0,1}]$ and $P_2[X_2\geq 1|MI_{0,2}]$ are the rack collapse probabilities due to overturning and buckling (defined by Eq. (1)); and $P_{L,k}$ is the vector sorted in descending order of the floor's failure probabilities $P_{l,i}$. The latter $P_{l,i}$ – i.e., the falling probability of containers from the i^{th} floor – and the number of simultaneous floor failures n_{FF} are given by:

$$n_{FF}(DS)=\left\lceil\left(\frac{H}{\Delta h_F}+1\right)\cdot Y_{DS}\right\rceil \qquad P_{l,i}=\begin{cases} P_4\left[X_4\geq 1\middle|MI_{0,4}\right] & i=0 \\ \max\limits_{j=3,4}\left(P_j\left[X_j\geq 1\middle|MI_{i,j}\right]\right) & i>0 \end{cases} \tag{3}$$

where H is the rack height; Δh_F is the inter-floor height; and Y_{DS} is a percentage that describes the loss intensity of rack containment (i.e., limit percentage of containers that fall from the frame: *DS0*=0%, *DS1*=30%, *DS2*=60%, and *DS3*=100%). The notation ⌈x⌉ indicates the smallest integer not less than x. $P_3[X_3\geq 1|MI_{i,3}]$ and $P_4[X_4\geq 1|MI_{i,4}]$ are the container falling probabilities due to sliding and overturning and $MI_{i,j}$ is the motion intensity at the i^{th} floor. Hence, the failure probability distribution $P_j[X_j\geq 1|MI_{i,j}]$ at the i^{th} floor and for the j^{th} damage mode is computed using Eq. (1). The ground motion intensity ($MI_{i,j}$) is measured with a dimensionless parameter, in order to increase the number of samples needed to fit the lognormal distributions and it is defined as follows:

$$MI_{i,j}=\frac{PFA_i}{a_{cr,j}} \tag{4}$$

where PFA_i is the median Peak Floor Acceleration; and $a_{cr,j}$ is defined as "critical horizontal acceleration" related to the j^{th} failure mechanism. In this study, the PFA_i is evaluated with a simplified procedure like that used in FEMA P-58 (FEMA, 2012). Analytically it is evaluated with a polynomial prediction equation given by:

$$\ln\left(\frac{PFA_i}{PGA}\right)=a_0+a_1\cdot h_i+a_2\cdot\frac{a_{cr,1}}{g}+a_3\cdot\frac{a_{cr,2}}{g} \quad \text{with } h_i=\Delta h_F\cdot i \tag{5}$$

where h_i is the height of the i^{th} floor; $a_{cr,1}$ and $a_{cr,2}$ are the critical horizontal accelerations for rack overturning (j=1) and the buckling (j=2) of the bracing system; and a_k are the regression coefficients. The critical horizontal accelerations will be discussed and explained in the following sections.

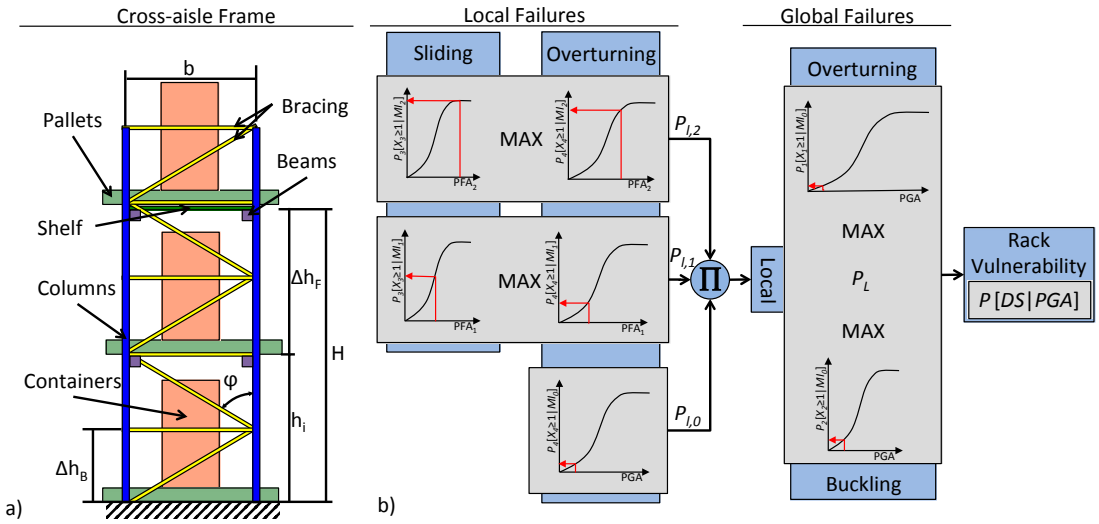

Figure 3. Cross-aisle frame configuration (a) and Fault tree model (b) adopted in this study.

The dataset of peak floor accelerations was evaluated summing the effects of the buckling and of the rocking models (Figure 4), under the presence of horizontal ground acceleration. The superposition of effects is valid if the cross-aisle frame does not slide, the rocking model has small rotation, and the cantilever has small elastic deformation. The details of the racking systems, the mathematical structural models, and the chosen seismic record are described in the following sections.

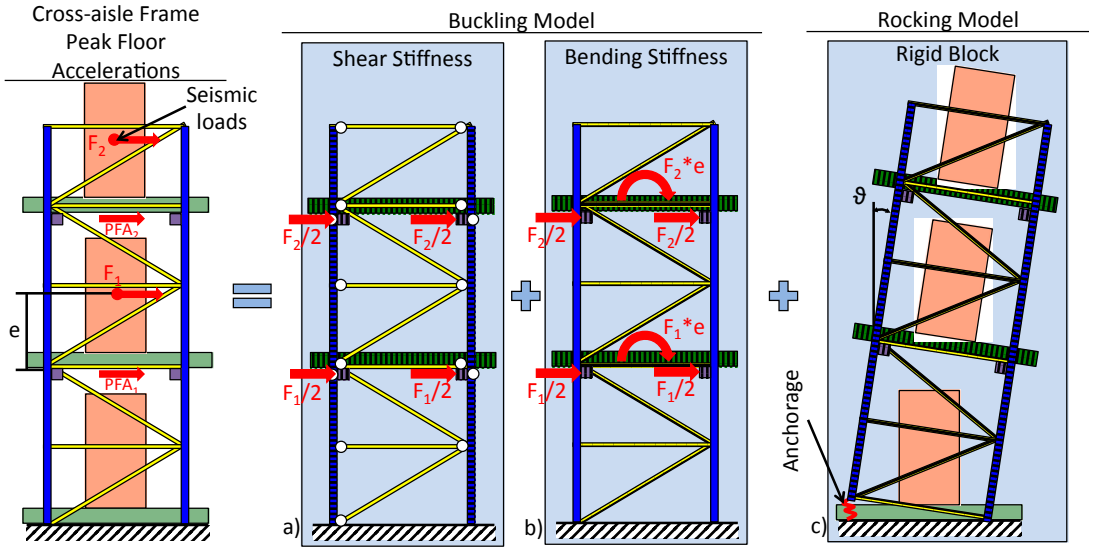

Figure 4. Cross-aisle frame mathematical models: buckling (a)+(b), and rocking (c).

3.1 Rocking model

This model studies the failure due to overturning of chemical containers and of the racking system in the cross-aisle direction considering the pure rocking mode (i.e., no slide) with impact and the effect of base anchorage. In a study of Makris and Zhang (1999), it was established that for earthquakes the effect of the vertical component of the ground motion is negligible with respect to the horizontal one in the rocking motion analysis. Moreover, it was demostrated that the restrainers are much more effective in preventing overturning for slender and smaller blocks. The racking system and containers were assumed as rigid blocks. The mathematical model considers that the rigid block – under the presence of horizontal ground acceleration – can oscillate about the centres of rotation *O* and *O'* when it is set to rocking (Figure 5).

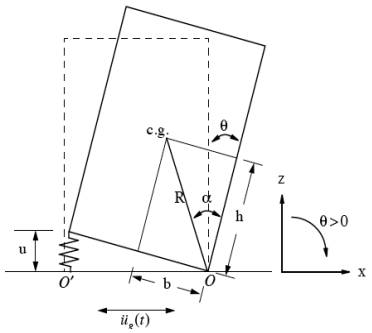

Figure 5. Schematic of an anchored block in rocking motion (Makris & Zhang, 1999).

Therefore, the equations that govern the rocking motion of the above-described model are the following (Makris & Zhang, 1999):

$$\begin{cases} \ddot{\vartheta} = -p^2 \cdot \left\{ \sin\left[\alpha \cdot \operatorname{sign}(\vartheta) - \vartheta\right] + \dfrac{\ddot{u}_g}{g} \cdot \cos\left(\alpha - |\vartheta|\right) \right\} - \ldots \\ \qquad - \dfrac{4 \cdot K_{el} \cdot R^2 \cdot \sin^2 \alpha}{I_0} \cdot \operatorname{sign}(\vartheta) \cdot f(\vartheta) \\ \dot{\vartheta}_{\text{after impact}} = \eta \cdot \dot{\vartheta}_{\text{before impact}} \\ p^2 = \dfrac{m \cdot g \cdot R}{I_0} \end{cases} \tag{6}$$

where ϑ is the rotation that describes the motion of the rigid block; I_0 and m is the moment of inertia about pivot point O or O' and the mass of the block, respectively; R is the distance between the centre of gravity and the centre of rotation; g is the gravity acceleration; α is the angle defined in Figure 5; $\ddot{u}_g$ is the ground acceleration; K_{el} is the elastic stiffness of the anchorage; $f(\vartheta)$ is a function that models the nonlinear hysteretic behaviour of the anchorage; $\dot{\vartheta}_{\text{after impact}}$ and $\dot{\vartheta}_{\text{before impact}}$ are the rotational velocity after and before the impact; η is the restitution coefficient; and p is the frequency parameter of the block. Note that the oscillation frequency of a rigid block under free vibration is not constant since it strongly depends on the vibration amplitude (Housner, 1963). Nevertheless, the quantity p is a measure of the dynamic characteristics and the limit capacity of the block.

Figure 6 illustrates the force-rotation relation of an anchorage with ductile behaviour. In general, the anchorage can exhibit a post-yielding stiffness and maintain its strength until it reaches the ultimate rotation. As mentioned above, the nonlinear hysteretic behaviour of the anchorage is analytically defined by the function $f(\vartheta)$ that was defined as follows:

$$f(\vartheta)=\begin{cases} k^*\cdot|\vartheta| & 0\le|\vartheta|<\vartheta_\chi \\ |\vartheta|+k^*\cdot\vartheta_\chi & \vartheta_\chi\le|\vartheta|\le\vartheta_\chi+\vartheta_Y \\ k^*\cdot(|\vartheta|-\vartheta_Y)+\vartheta_Y & \vartheta_\chi+\vartheta_Y<|\vartheta|<\vartheta_U\cdot H(\vartheta_\chi) \\ 0 & |\vartheta|\ge\vartheta_U\cdot H(\vartheta_\chi) \end{cases} \quad \text{with} \quad \begin{cases} \chi=\text{sign}(\vartheta) \\ k^*=\dfrac{K_{pl}}{K_{el}} \end{cases} \tag{7}$$

where K_{pl} is the plastic stiffness of the anchorage; ϑ_Y is the elastic rotation; ϑ_U is the ultimate rotation; H is the Heaviside function; and ϑ_χ is a variable (see Figure 6) that changes on each integration step and it is analytically defined as follows:

$$\vartheta_\chi^+=\begin{cases} |\vartheta|\cdot H(-\dot{\vartheta}\cdot\chi)+\left[1-H(-\dot{\vartheta}\cdot\chi)\right]\cdot\vartheta_\chi^- & 0\le|\vartheta|<\vartheta_\chi^- \\ \vartheta_\chi^- & \vartheta_\chi^-\le|\vartheta|\le\vartheta_\chi^-+\vartheta_Y \\ (|\vartheta|-\vartheta_Y)\cdot H(\dot{\vartheta}\cdot\chi)+\left[1-H(\dot{\vartheta}\cdot\chi)\right]\cdot\vartheta_\chi^- & \vartheta_\chi^-+\vartheta_Y<|\vartheta|\le\vartheta_U\cdot H(\vartheta_\chi^-) \\ -\vartheta_U & |\vartheta|>\vartheta_U\cdot H(\vartheta_\chi^-) \end{cases} \tag{8}$$

where ϑ_χ^- and ϑ_χ^+ are the values of the variable before and after the integration step.

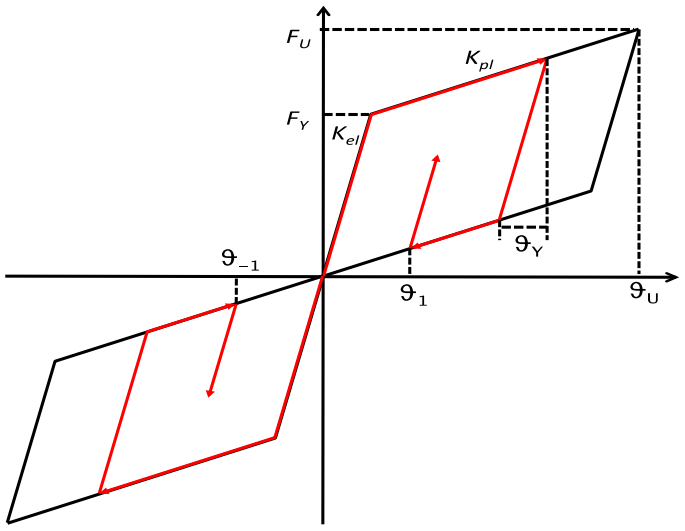

Figure 6. Anchorage plastic behaviour.

In this study, in order to consider model and integration errors, the failure (i.e., overturning) of the rigid block occurs when the rotation reaches 90% of the angle α, or in other words, when the gravity load, i.e. the "stiffness" that returns the system to the initial state, becomes close to zero. Thus, the parameter that describes the overturning (X_1 and X_4), i.e. the failure of the rigid block, is defined as:

$$X_j = \frac{\max\left|\vartheta(t)\right|}{\alpha \cdot 0.9} \text{ with } j = 1 \text{ or } 4 \tag{9}$$

where $\vartheta(t)$ is the rotation of the rigid block at time t evaluated integrating Eq. (6).

In order to compare the anchorage types, the static horizontal acceleration $a_{st,j}$ needed to break the anchorage was evaluated as follows:

$$a_{st,j} = \frac{2 \cdot \sin(\alpha) \cdot F_{cr}(\vartheta_{cr})}{m \cdot \cos(\alpha - \vartheta_{cr})} + g \cdot \tan(\alpha - \vartheta_{cr}) \quad \text{with} \quad \begin{cases} j = 1 \text{ or } 4 \\ 0 \le \vartheta_{cr} \le \vartheta_U \end{cases} \tag{10}$$

where ϑ_{cr} is defined as the "critical rotation" that maximises the value of $a_{st,j}$; and $F_{cr}(\vartheta_{cr})$ is defined as the "equivalent anchorage strength". The latter, in case of elastic-plastic behaviour, implicitly defines an equivalent model with brittle behaviour that has the same strain energy of the elastic-plastic model at ϑ_{cr} and it is given by:

$$F_{cr}(\vartheta_{cr}) = \begin{cases} K_{el} \cdot \vartheta_{cr} & \vartheta_{cr} \le \vartheta_Y \\ \dfrac{F_Y}{\vartheta_{cr}} \cdot \left\{ \vartheta_{cr} + \left[1 + \dfrac{K_{pl}}{F_Y} \cdot (\vartheta_{cr} - \vartheta_Y) \right] \cdot (\vartheta_{cr} - \vartheta_Y) \right\} & \vartheta_{cr} > \vartheta_Y \end{cases} \tag{11}$$

In order to compare the results of anchored with unanchored blocks, an equivalent model was defined. This model consists of an equivalent unanchored rectangular block that has the same mass and dissipates the same amount of energy when the block reaches the critical rotation ($\vartheta = \vartheta_{cr}$) and the verge of overturning ($\vartheta = \alpha$) with respect to the anchored model with elastic-brittle behaviour. The energy is evaluated assuming that at the verge of overturning and at the critical rotation, the kinetic energy of the block is zero, i.e. it is assumed that the earthquake excitation is terminated. The parameters that describe the equivalent model are given by:

$$\begin{cases} R_{eq} = R \cdot \left[1 + \dfrac{F_{cr}(\vartheta_{cr}) \cdot \vartheta_{cr} \cdot \sin\alpha}{m \cdot g \cdot (1 - \cos\vartheta_{cr})} \right] \\ \alpha_{eq} = \operatorname{acos}\left\{ 1 - (1 - \cos\alpha) \cdot \dfrac{\left[1 + \dfrac{F_{cr}(\vartheta_{cr}) \cdot \vartheta_{cr} \cdot \sin\alpha}{m \cdot g \cdot (1 - \cos\alpha)} \right]}{\left[1 + \dfrac{F_{cr}(\vartheta_{cr}) \cdot \vartheta_{cr} \cdot \sin\alpha}{m \cdot g \cdot (1 - \cos\vartheta_{cr})} \right]} \right\} \end{cases} \tag{12}$$

As indicated before, the frequency parameter p is a measure of the dynamic characteristics and the limit capacity of the block. For rectangular blocks, $p^2 = 3g/4R$, i.e. the larger the block (larger R), the smaller is p and the smaller is the probability of failure $P_j[X_j \ge 1 | MI_{i,j}]$. Hence, to consider geometrical and scale effects, the minimum static acceleration needed to initiate the rocking of the equivalent unanchored rectangular block is divided by its frequency parameter p as follows:

$$a_{cr,j} = \frac{g \cdot \tan\alpha_{eq}}{\sqrt{\dfrac{3 \cdot g}{4 \cdot R_{eq}}}} \tag{13}$$

3.2 Sliding model

This model studies the falling of chemical containers from the rack floors considering the pure sliding mode. The system is modelled as the SDOF sliding system described by Denoël and Degee (2005) and is defined as follows:

$$\begin{cases} \ddot{u} = \ddot{u}_g & \left|\ddot{u}_g\right| < a_{cr,3} \ \text{ and } \ \Delta v = 0 \\ \ddot{u} = \mu_d \cdot g \cdot \left\{ \text{sign}\left(\Delta v\right) + \left[1 - \left|\text{sign}\left(\Delta v\right)\right|\right] \cdot \text{sign}\left(\ddot{u}_g\right) \right\} & \left|\ddot{u}_g\right| \geq a_{cr,3} \ \text{ or } \ \Delta v \neq 0 \end{cases} \tag{14}$$

where μ_S and μ_d are the static and dynamic friction coefficients; u is the mass displacement; $a_{cr,3}$, Δu and Δv are, respectively, the critical horizontal acceleration needed to initiate sliding, and the relative displacement and velocity between the mass and the support that are given by:

$$a_{cr,3} = g \cdot \mu_S \quad \Delta v = \dot{u}_g - \dot{u} \quad \Delta u = u_g - u \tag{15}$$

The failure of the rigid block (i.e., when a container drops from its rack floor) occurs when the rigid block reaches the limit of relative displacement. Thus, the parameter that describes the failure for sliding (X_3) is defined as:

$$X_3 = \frac{\max\left|\Delta u(t)\right|}{\Delta u_{Lim}} \tag{16}$$

where Δu_{Lim} is the relative displacement limit.

3.3 Buckling model

This model studies the failure of the first floor of racking system in the cross-aisle direction due to the buckling of the diagonal bracing at the ground floor. The system is modelled as a cantilever with lumped masses superposing the effects of bending and shear flexibility as shown in Figure 4. The equations that govern the dynamic motion are the following (Chopra, 1995):

$$\begin{bmatrix} m_1 & \cdots & 0 \\ \vdots & \ddots & \vdots \\ 0 & \cdots & m_n \end{bmatrix} \left(\left\{\ddot{u}\right\} + \left\{\ddot{u}_g\right\} \right) + \left[C\right]\left\{\dot{u}\right\} + \left(\left[K_S\right]^{-1} + \left[K_B\right]^{-1} \right)^{-1} \left\{u\right\} = \left\{0\right\} \tag{17}$$

where m_i are the floor masses; $\{u\}$ is the vector of the floor horizontal displacements; $[C]$ is the damping matrix; and $[K_S]$ and $[K_B]$ are the stiffness matrices of the racking system considering the shear and the bending flexibilities. The bending stiffness matrix is evaluated assuming the structural model shown in Figure 4b and the inertia I of the cantilever beam:

$$I = \left(\frac{A_C}{2} \cdot b^2 + 2 \cdot I_C \right) \tag{18}$$

where b is the inter-column distance in the cross-aisle direction (Figure 3a); and A_C and I_C are the area and the inertia of the upright columns. The shear stiffness matrix is evaluated assuming the structural model shown in Figure 4a and is analytically defined as follows:

$$\left[K_S\right] = k_S \cdot \begin{bmatrix} 2 & -1 & 0 & \cdots & 0 \\ -1 & 2 & -1 & \cdots & 0 \\ 0 & -1 & 2 & \cdots & 0 \\ \vdots & \vdots & \vdots & \ddots & -1 \\ 0 & 0 & 0 & -1 & 1 \end{bmatrix} \quad \text{with} \quad k_S = \frac{E_B \cdot A_B}{\Delta h_F} \cdot \left(\frac{b}{\Delta h_B} + \frac{1}{\cos\varphi \cdot \sin^2\varphi} \right)^{-1} \tag{19}$$

where A_B and E_B are the area and the elastic modulus of the bracing trusses; φ is the angle defined in Figure 3a; and k_S is the floor bracing stiffness. The maximum axial load N_{MAX} due to the seismic ground motion, and the critical buckling load N_{cr} – assuming a buckling length factor equal to 0.5 – acting on the diagonal bracing truss of the first floor are given by:

$$N_{MAX} = E_B \cdot A_B - \frac{E_B \cdot A_B \cdot \cos\varphi}{\cos\left[\operatorname{atan}\left(\tan\varphi - \frac{F_{1,MAX} \cdot \cos^{-1}\varphi \cdot \sin^{-2}\varphi}{E_B \cdot A_B}\right)\right]} \quad N_{cr} = E_B \cdot I_B \cdot \left(\frac{\pi \cdot \cos\varphi}{0.5 \cdot \Delta h_B}\right)^2 \tag{20}$$

where I_B is the inertia of the diagonal truss; $F_{1,MAX}$ is the maximum absolute elastic force at the first floor evaluated with Eq. (17); and Δh_B is the "span" of the bracing system assuming a K-form. Besides, the critical acceleration needed to initiate the buckling at the first floor was defined as follows:

$$a_{cr,2} = \frac{E_B \cdot A_B \cdot \Delta h_B}{\sum_i m_i \cdot \Delta h_F \cdot i} \cdot \sin^2\varphi \cdot \left(\sin\varphi - \cos\varphi \cdot \tan\varphi_{cr}\right) \text{ with } \cos\varphi_{cr} = \frac{\cos\varphi}{1 - \frac{N_{cr}}{E_B \cdot A_B}} \tag{21}$$

In this study, in order to consider the non-linear behaviour of the bracing system, the racking system's failure due to the buckling of the diagonal bracing at the ground floor is defined when the maximum axial load N_{MAX} (reduced by 10% to consider model and integration errors) exceeds the critical buckling load N_{cr}. Thus, the parameter that describes the buckling failure (X_2) is defined as:

$$X_2 = \frac{N_{MAX} \cdot 0.90}{N_{cr}} \tag{22}$$

4 Numerical Results

As indicated in the previous sections, the typical containers used in chemical warehouses are IBCs and metal drums. In this study, drums are assumed stacked to no more than four on a wooden pallet, which is located over a shelf (i.e., a surface that is the load level of the rack floor that, in this study, is composed of steel panels pinned on the beams of the rack, see Figure 3a). The IBCs have a plastic basement and are placed directly on the beams of the rack. The presence or absence of the shelf affects the limit states (i.e., the relative displacement limits Δu_{Lim}) for the sliding of the containers (Table 1).

Rigid Block Type	μ_S [-]	μ_d [-]	Δu_{Lim} [m]
4 Drums on Wooden Pallet	0.5	0.14	0.4
IBC	0.2	0.1	0.2

Table 1. Friction properties (Castiglioni et al., 2008) and displacement limits used for the study for chemical containers.

The characteristics of standard containers used in the present study are shown in Table 2.

Container Type	V [L]	Self weight [kg]	H [mm]	B [mm]	W [mm]
Steel Drum	200	20.2	876	587	587
IBC (with plastic pallet)	1000	59	1160	1000	1200
"Philips" Wooden Pallet	-	18.5	144	1000	1200

Table 2. Dimensions and weights of standard containers (ANSI, 1997; D'Hollander, 1993; NWPCA, 1996).

In the present study, racking systems with constant bays (1 m deep and 2.2 m wide; i.e. two pallets per bay) and different heights (H= 3, 4.5, 6, 7.5, 9 m) with a constant inter-floor height Δh_F of 1.5 m were studied. More than 23,000 random combinations changing the density of chemical substance and the strength of the anchorage were considered. The set of combinations used had an average density of chemical substance of about 710 kg/m^3 with a standard deviation (s.d.) of about 30%. To consider the spatial distribution of the containers and the worst-case scenario, it is assumed that during the earthquake the racking systems are 80% loaded with containers. For the braced frame we assumed a K-form and a "span" Δh_B of 0.65 m (see Figure 3a). The bracing system's elements were assumed with cross-sections of 41 x 20.6 x 1.9mm (i.e., half solid channel), while the upright columns have a section 100/20b (Castiglioni, 2008). The latter can support loads of up to 95 kN, using a safety coefficient of 1.92. The base plate is connected to the foundation surface (when anchoring configuration is assumed) by means of two M16 (grade 8.8) bolts. The ultimate strength is evaluated using a safety coefficient of 1.2 (Eurocode 3). Geometrical properties and material characteristics of frame elements are reported in Table 3.

Element Type	A	I	E	F_y	F_u	ε_u
[-]	[mm^2]	[mm^4]	[GPa]	[MPa]	[MPa]	[-]
Column	525.7	406100	210	348	493	25.5%
Bracing Truss	187.1	45000	210	348	493	25.5%
M16 (grade 8.8) bolts	157.0	-	-	-	667	-

Table 3. Geometrical properties and material characteristics of rack elements (Castiglioni, 2008).

The reliability of the simplified structural model (i.e., buckling model) is confirmed by fundamental periods of vibration in the cross-aisle direction of the analysed racking systems that range from 0.17-0.72 s like those found in the literature (Castiglioni, 2008).

Rack Height [m]	3	4.5	6	7.5	9
Mean Period [s]	0.170	0.296	0.432	0.538	0.722
Standard deviation [-]	19%	18%	12%	19%	17%

Table 4. Fundamental periods in the cross-aisle direction of the analysed racking systems.

In accordance with the literature, a damping ratio of 2% and a restitution coefficient η equal to 0.9 were assumed for the dynamic analysis of the buckling and rocking models (Makris & Zhang, 1999). The properties of rigid blocks analysed with the rocking and sliding models are given in the Table 5. The chemical containers were assumed as unanchored, while the racking systems were studied under the assumption of three different anchorage types. When the racking system is free to rotate into the cross-aisle direction the anchorage type is "unanchored", while it is "anchored" if the base is fastened to the floor with bolts.

Rigid Block Type	α		m		I_0		R	
	mean	s.d.	mean	s.d.	mean	s.d.	mean	s.d.
	[rad]	[-]	[kg]	[-]	[kg*m^2]	[-]	[m]	[-]
IBC	0.725	0%	804.67	33%	678	33%	0.754	0%
Drum	0.627	0%	168.59	32%	53	32%	0.503	0%
Rack (H=3)	0.283	27%	2594.09	35%	22551	35%	2.883	1%
Rack (H=4.5)	0.227	27%	3670.79	35%	52879	35%	3.619	1%
Rack (H=6)	0.189	28%	5100.54	27%	110244	27%	4.359	0%
Rack (H=7.5)	0.162	28%	5634.40	31%	170801	31%	5.102	0%
Rack (H=9)	0.142	28%	6755.18	28%	273867	28%	5.848	0%

Table 5. Properties of the analysed rigid blocks.

The anchorage's behaviour is considered "brittle" when the strength of the bolts is lower than that of the upright column; vice versa it is considered "plastic". The characteristics of the anchorage types analysed are given in Table 6 (these are derived from the geometrical properties and material characteristics of racking system in Table 3).

Anchorage Type	F_Y		F_U		ϑ_Y		ϑ_U	
	mean [kN]	s.d. [-]	mean [kN]	s.d. [-]	mean [rad]	s.d. [-]	mean [rad]	s.d. [-]
Anchored-Plastic	201	34%	279	34%	0.0027	0%	0.3825	0%
Anchored-Brittle	287	25%	-	-	0.0025	-	-	-
Unanchored	-	-	-	-	-	-	-	-

Table 6. Properties of the analysed anchorage type blocks.

4.1 Ground motion records

Details of a set of ground motion records, which were used as the general set for the collapse fragility assessment of rack elements, are presented in Table 7. This general set, which includes 26 records, was obtained from the PEER Strong Motion database (http://peer.berkeley.edu/smcat/search.html). The records are from a variety of different geological sites including rock and soft soil conditions. The peak ground acceleration ranges from 0.45-1.78 g with a mean value of 0.89 g and a s.d. of 38%.

Record ID	Earthquake	Record/Component	M [-]	D [km]	PGA [g]	PGV [cm/s]	PGD [cm]
P0806	Cape Mendocino 1992/04/25	CAPEMEND/CPM000	7.1	8.5	1.50	127	41.0
P1455	Chi-Chi, Taiwan 1999/09/20	CHICHI/TCU084-W	7.6	10.4	1.16	115	31.4
P1169	Chi-Chi, Taiwan 1999/09/20	CHICHI/CHY080-W	7.6	7.0	0.97	108	18.6
P1532	Chi-Chi, Taiwan 1999/09/20	CHICHI/WNT-E	7.6	1.2	0.96	69	31.1
P0409	Coalinga 1983/07/22	COALINGA/D-OLC270	5.8	8.2	0.87	42	6.1
P0414	Coalinga 1983/07/22	COALINGA/D-TSM360	5.8	9.2	1.08	40	5.4
P1547	Duzce, Turkey 1999/11/12	DUZCE/BOL090	7.1	17.6	0.82	62	13.6
P0127	Gazli, USSR 1976/05/17	GAZLI/GAZ090	6.8	3.0	0.72	72	23.7
P0178	Imperial Valley 1979/10/15	IMPVALL/H-E06230	6.5	1.0	0.44	110	65.9
P1056	Kobe 1995/01/16	KOBE/TAZ090	6.9	1.2	0.69	85	16.8
P0873	Landers 1992/06/28	LANDERS/LCN275	7.3	1.1	0.72	98	70.3
P0760	Loma Prieta 1989/10/18	LOMAP/BRN090	6.9	10.3	0.45	51	8.4
P0770	Loma Prieta 1989/10/18	LOMAP/LGP000	6.9	6.1	0.56	95	41.2
P0449	Morgan Hill 1984/04/24	MORGAN/CYC285	6.2	0.1	1.30	81	9.6
P0496	Nahanni, Canada 1985/12/23	NAHANNI/S1280	6.8	6.0	1.10	46	14.6
P0935	Northridge 1994/01/17	NORTHR/TAR090	6.7	17.5	1.78	114	33.2
P0996	Northridge 1994/01/17	NORTHR/PUL194	6.7	8.0	1.29	104	23.8
P0530	N. Palm Springs 1986/07/08	PALMSPR/NPS210	6.0	8.2	0.59	73	11.5
P0144	Tabas, Iran 1978/09/16	TABAS/TAB-TR	7.4	3.0	0.85	121	94.6
P0266	Victoria, Mexico 1980/06/09	VICT/CPE045	6.4	34.8	0.62	32	13.2
P0319	Westmorland 1981/04/26	WESTMORL/WSM180	5.8	13.3	0.50	34	10.9
P0701	Whittier Narrows 1987/10/01	WHITTIER/A-TAR090	6.0	43.0	0.64	23	1.7
P0082	San Fernando 1971/02/09	SFERN/PCD164	6.6	2.8	1.23	113	35.5
P0248	Mammoth Lakes 1980/05/27	MAMMOTH/L-LUL000	6.0	20.0	0.92	29	3.2
P0802	Erzincan, Turkey 1992/03/13	ERZIKAN/ERZ-NS	6.9	2.0	0.52	84	27.4
P0161	Imperial Valley 1979/10/15	IMPVALL/H-BCR230	6.5	2.5	0.78	46	14.9

Table 7. Details of a set of ground motion records (where M is the magnitude; D is the distance between the station and the earthquake source; PGV and PGD are the peak ground velocities and displacements).

4.2 Fragility curves

Utilizing the results of nonlinear dynamic analyses with the models presented above under the selected ground-motion forces, the polynomial regression coefficients of Eq. (5) and the lognormal fragility curve parameters (see Eq. (1)) were estimated by using the least squares method. Table 8 shows the regression coefficients for the analysed racks and the coefficient of determination R^2.

Height Range [m]	a_0 [-]	a_1 [-]	a_2 [-]	a_3 [-]	R^2 [-]	N° [-]
3 - 9	-0.091	0.189	0.065	0.655	51%	32254

Table 8. Regression coefficients of the *PFA* prediction equation(5).

The four fragility curves (blue lines) fitted to the analytical datasets (red triangles) are depicted in Figure 7 with the weight coefficients of the bins (green bars) adopted to fit cumulative lognormal models.

Table 9 shows the lognormal distribution parameters for overturning, sliding, and buckling failures, the coefficient of determination R^2, the number of simulations N°, and the application domain of the proposed formulas. The parameters were estimated with a generalized linear regression with a Probit link function to predict the probability of collapse as a function of ln(*MI*) (Agresti, 2012). Generalized linear regression uses maximum likelihood for estimation and the Probit link function is equivalent to using the normal cumulative distribution function as the fragility function.

Failure Mode	σ [-]	μ [-]	R^2 [-]	N° [-]	*MI* Domain [-]
Overturning	0.75	15.51	96%	51454	0.5-70
Buckling	0.60	4.91	92%	7800	0.077-18
Sliding - Δu_{Lim} = 0.2 m	1.01	3.02	96%	31252	0.729-45
Sliding - Δu_{Lim} = 0.4 m	1.03	6.72	97%	31252	0.729-45

Table 9. Fragility curve parameters for overturning, buckling, and sliding modes.

It is worth noting that the simulations for chemical containers were performed with ground and floor accelerations, derived from the buckling model, while those of the racking system were carried out only with ground accelerations. Table 10 shows the number n_{FF} of simultaneous floor failures defined for the selected rack heights.

H [m] \ Y_{DS} [-]	30%	60%	100%
3	1	2	3
4.5	2	3	4
6	2	3	5
7.5	2	4	6
9	3	5	7

Table 10. Number n_{FF} of simultaneous floor failures.

Table 11, Table 12, Figure 8, and Figure 9 show the probabilities of being in or exceeding a given damage state (*DS*) – evaluated with Eq. (2) – for eighteen types of racking systems loaded with drums and IBCs. The chemical containers are assumed to be filled with a chemical substance that has a density of about 710 kg/m^3 (e.g., gasoline). The eighteen types of racking systems differ in height (H = 3, 4.5, 6, 7.5, and 9 m) and anchorage type (unanchored, anchored-brittle, and anchored-plastic). The structural characteristics of the racking system (i.e., sections, inertias, bolts, etc.) have been assumed according to mechanical features described in Table 1, Table 2 and Table 3.

The obtained analytical fragility curves exhibit a higher level of total falling probability (i.e., *DS3*) with increasing rack height and the decreasing of the robustness of the anchorage. At the same time, the falling probability of containers (i.e., *DS1* and *DS2*) decreases with respect to the decreasing of the robustness of the anchorage. This effect is due to the reduction of the *PFA* intensity. Racks loaded with IBCs showed a higher level of falling probability of containers compared with those loaded with drums, due to the lower friction coefficient and the higher weight.

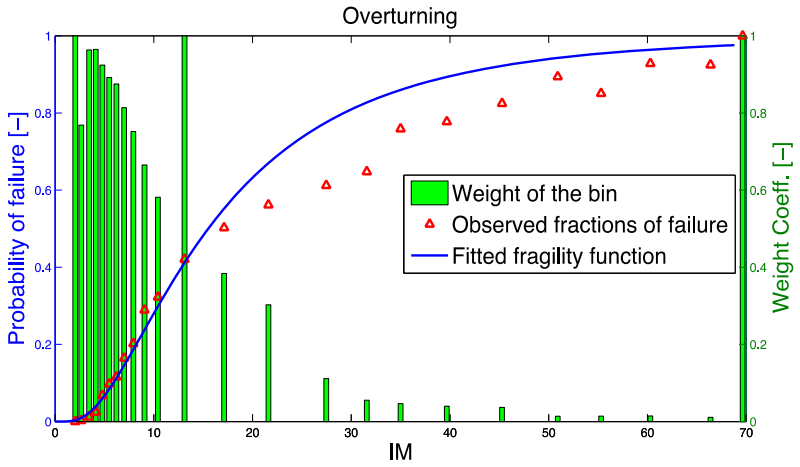
Overturning
Probability of failure [–]
Weight Coeff. [–]
IM
Weight of the bin
Observed fractions of failure
Fitted fragility function

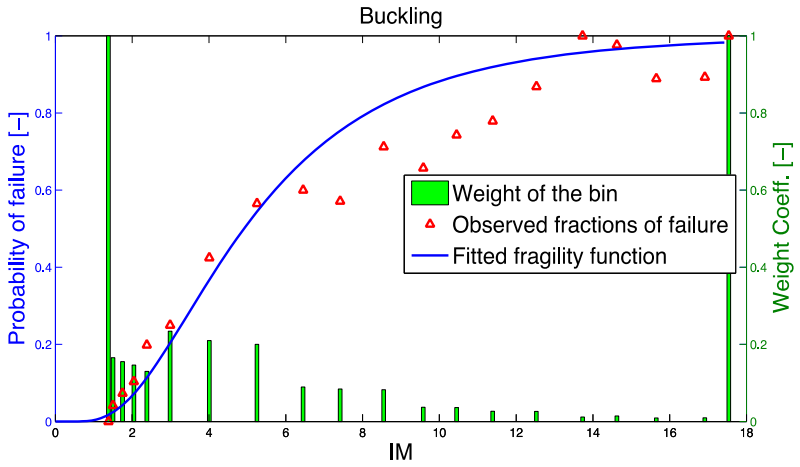
Buckling
Probability of failure [–]
Weight Coeff. [–]
IM
Weight of the bin
Observed fractions of failure
Fitted fragility function

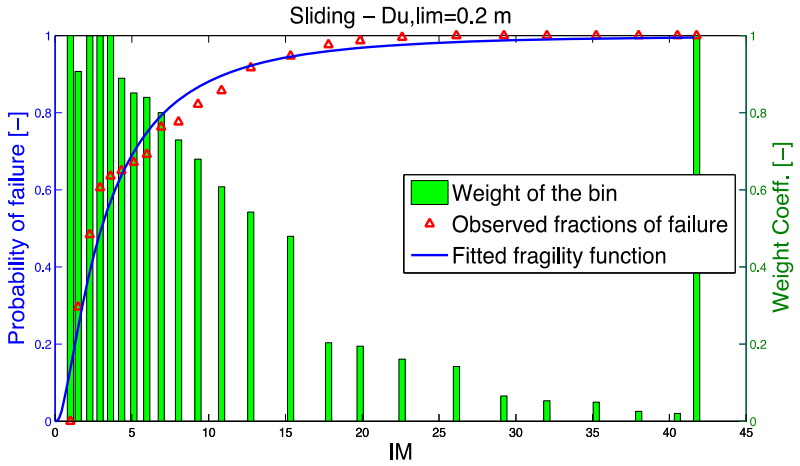
Sliding – Du,lim=0.2 m
Probability of failure [–]
Weight Coeff. [–]
IM
Weight of the bin
Observed fractions of failure
Fitted fragility function

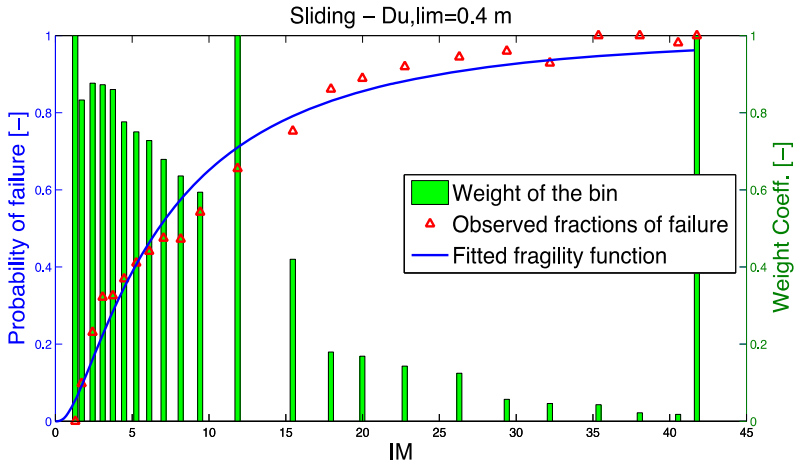
Sliding – Du,lim=0.4 m
Probability of failure [–]
Weight Coeff. [–]
IM
Weight of the bin
Observed fractions of failure
Fitted fragility function

Rack Type \ P GA [g]	0	0.1	0.2	0.3	0.4	0.5	0.6	0.7	0.8	0.9	1	1.1	1.2	1.3	1.4	1.5
Anchored-Brittle & H=3m-DS1	0%	0%	2%	5%	9%	12%	16%	20%	24%	28%	32%	36%	41%	45%	49%	52%
Anchored-Brittle & H=3m-DS2	0%	0%	0%	1%	2%	4%	6%	9%	12%	15%	19%	22%	26%	29%	33%	36%
Anchored-Brittle & H=3m-DS3	0%	0%	0%	1%	2%	4%	6%	9%	12%	15%	19%	22%	26%	29%	33%	36%
Anchored-Brittle & H=4.5m-DS1	0%	0%	0%	1%	3%	5%	8%	12%	16%	20%	24%	28%	32%	36%	40%	43%
Anchored-Brittle & H=4.5m-DS2	0%	0%	0%	1%	3%	5%	8%	12%	16%	20%	24%	28%	32%	36%	40%	43%
Anchored-Brittle & H=4.5m-DS3	0%	0%	0%	1%	3%	5%	8%	12%	16%	20%	24%	28%	32%	36%	40%	43%
Anchored-Brittle & H=6m-DS1	0%	0%	0%	2%	4%	7%	11%	15%	19%	24%	28%	33%	37%	41%	45%	49%
Anchored-Brittle & H=6m-DS2	0%	0%	0%	2%	4%	7%	11%	15%	19%	24%	28%	33%	37%	41%	45%	49%
Anchored-Brittle & H=6m-DS3	0%	0%	0%	2%	4%	7%	11%	15%	19%	24%	28%	33%	37%	41%	45%	49%
Anchored-Brittle & H=7.5m-DS1	0%	0%	0%	2%	5%	8%	13%	18%	23%	30%	36%	42%	47%	52%	57%	61%
Anchored-Brittle & H=7.5m-DS2	0%	0%	0%	2%	5%	8%	13%	18%	23%	28%	32%	37%	42%	46%	50%	53%
Anchored-Brittle & H=7.5m-DS3	0%	0%	0%	2%	5%	8%	13%	18%	23%	28%	32%	37%	42%	46%	50%	53%
Anchored-Brittle & H=9m-DS1	0%	0%	1%	3%	6%	10%	15%	20%	26%	31%	36%	41%	45%	50%	54%	57%
Anchored-Brittle & H=9m-DS2	0%	0%	1%	3%	6%	10%	15%	20%	26%	31%	36%	41%	45%	50%	54%	57%
Anchored-Brittle & H=9m-DS3	0%	0%	1%	3%	6%	10%	15%	20%	26%	31%	36%	41%	45%	50%	54%	57%
Anchored-Plastic & H=3m-DS1	0%	2%	8%	15%	23%	30%	38%	46%	53%	59%	65%	69%	73%	77%	79%	82%
Anchored-Plastic & H=3m-DS2	0%	0%	0%	1%	4%	6%	10%	15%	20%	26%	32%	38%	44%	49%	53%	58%
Anchored-Plastic & H=3m-DS3	0%	0%	0%	0%	0%	0%	0%	0%	1%	2%	2%	4%	5%	7%	9%	11%
Anchored-Plastic & H=4.5m-DS1	0%	0%	0%	2%	4%	8%	12%	18%	24%	30%	37%	43%	48%	53%	58%	62%
Anchored-Plastic & H=4.5m-DS2	0%	0%	0%	0%	0%	1%	2%	4%	7%	10%	14%	19%	23%	28%	33%	37%
Anchored-Plastic & H=4.5m-DS3	0%	0%	0%	0%	0%	0%	0%	0%	0%	1%	1%	2%	3%	4%	5%	7%
Anchored-Plastic & H=6m-DS1	0%	0%	1%	3%	7%	12%	18%	26%	34%	41%	48%	54%	59%	64%	68%	72%
Anchored-Plastic & H=6m-DS2	0%	0%	0%	0%	1%	2%	5%	8%	12%	17%	23%	28%	34%	39%	45%	49%
Anchored-Plastic & H=6m-DS3	0%	0%	0%	0%	0%	0%	0%	0%	0%	1%	1%	2%	3%	3%	4%	6%
Anchored-Plastic & H=7.5m-DS1	0%	0%	1%	3%	6%	10%	16%	23%	30%	37%	44%	50%	55%	60%	65%	69%
Anchored-Plastic & H=7.5m-DS2	0%	0%	0%	0%	0%	0%	1%	1%	2%	4%	6%	9%	12%	15%	19%	23%
Anchored-Plastic & H=7.5m-DS3	0%	0%	0%	0%	0%	0%	1%	1%	2%	4%	5%	7%	9%	12%	14%	17%
Anchored-Plastic & H=9m-DS1	0%	0%	0%	1%	2%	4%	8%	14%	20%	26%	33%	40%	46%	51%	56%	61%
Anchored-Plastic & H=9m-DS2	0%	0%	0%	0%	0%	1%	3%	5%	7%	10%	14%	18%	22%	26%	30%	34%
Anchored-Plastic & H=9m-DS3	0%	0%	0%	0%	0%	1%	3%	5%	7%	10%	14%	18%	22%	26%	30%	34%
Unanchored & H=3m-DS1	0%	0%	2%	5%	8%	12%	16%	20%	24%	28%	31%	36%	40%	44%	48%	52%
Unanchored & H=3m-DS2	0%	0%	0%	1%	3%	5%	8%	12%	15%	19%	24%	28%	32%	35%	39%	43%
Unanchored & H=3m-DS3	0%	0%	0%	1%	3%	5%	8%	12%	15%	19%	24%	28%	32%	35%	39%	43%
Unanchored & H=4.5m-DS1	0%	0%	0%	2%	4%	7%	11%	15%	20%	24%	29%	33%	38%	42%	45%	49%
Unanchored & H=4.5m-DS2	0%	0%	0%	2%	4%	7%	11%	15%	20%	24%	29%	33%	38%	42%	45%	49%
Unanchored & H=4.5m-DS3	0%	0%	0%	2%	4%	7%	11%	15%	20%	24%	29%	33%	38%	42%	45%	49%
Unanchored & H=6m-DS1	0%	0%	1%	2%	5%	9%	13%	18%	23%	28%	33%	38%	42%	47%	51%	54%
Unanchored & H=6m-DS2	0%	0%	1%	2%	5%	9%	13%	18%	23%	28%	33%	38%	42%	47%	51%	54%
Unanchored & H=6m-DS3	0%	0%	1%	2%	5%	9%	13%	18%	23%	28%	33%	38%	42%	47%	51%	54%
Unanchored & H=7.5m-DS1	0%	0%	1%	3%	6%	11%	16%	21%	27%	32%	37%	42%	47%	52%	57%	61%
Unanchored & H=7.5m-DS2	0%	0%	1%	3%	6%	11%	16%	21%	27%	32%	37%	42%	47%	51%	55%	59%
Unanchored & H=7.5m-DS3	0%	0%	1%	3%	6%	11%	16%	21%	27%	32%	37%	42%	47%	51%	55%	59%
Unanchored & H=9m-DS1	0%	0%	1%	3%	7%	12%	18%	24%	30%	36%	41%	46%	50%	55%	59%	62%
Unanchored & H=9m-DS2	0%	0%	1%	3%	7%	12%	18%	24%	30%	36%	41%	46%	50%	55%	59%	62%
Unanchored & H=9m-DS3	0%	0%	1%	3%	7%	12%	18%	24%	30%	36%	41%	46%	50%	55%	59%	62%

Table 11. Numerical values of probabilities of being in or exceeding a given *DS* for racking systems loaded with drums.

Rack Type \ P GA [g]	0	0.1	0.2	0.3	0.4	0.5	0.6	0.7	0.8	0.9	1	1.1	1.2	1.3	1.4	1.5
Anchored-Brittle & H=3m-DS1	0%	14%	34%	50%	61%	69%	75%	80%	83%	86%	88%	90%	91%	92%	93%	94%
Anchored-Brittle & H=3m-DS2	0%	1%	8%	19%	30%	40%	49%	56%	62%	68%	72%	75%	78%	81%	83%	85%
Anchored-Brittle & H=3m-DS3	0%	0%	0%	1%	2%	4%	6%	9%	12%	16%	20%	23%	27%	31%	34%	37%
Anchored-Brittle & H=4.5m-DS1	0%	2%	13%	27%	40%	50%	59%	66%	71%	76%	79%	82%	85%	87%	89%	90%
Anchored-Brittle & H=4.5m-DS2	0%	0%	3%	10%	19%	28%	37%	45%	52%	58%	63%	68%	71%	75%	78%	80%
Anchored-Brittle & H=4.5m-DS3	0%	0%	0%	1%	3%	5%	9%	12%	16%	21%	25%	29%	33%	37%	41%	44%
Anchored-Brittle & H=6m-DS1	0%	5%	21%	38%	52%	62%	70%	76%	80%	84%	87%	89%	90%	92%	93%	94%
Anchored-Brittle & H=6m-DS2	0%	1%	6%	17%	29%	40%	50%	58%	64%	70%	74%	78%	81%	83%	86%	87%
Anchored-Brittle & H=6m-DS3	0%	0%	0%	2%	4%	7%	11%	15%	20%	25%	29%	34%	38%	42%	46%	50%
Anchored-Brittle & H=7.5m-DS1	0%	9%	32%	51%	64%	73%	79%	84%	87%	90%	92%	93%	95%	95%	96%	97%
Anchored-Brittle & H=7.5m-DS2	0%	0%	4%	13%	24%	35%	45%	53%	61%	66%	71%	75%	79%	82%	84%	86%
Anchored-Brittle & H=7.5m-DS3	0%	0%	1%	2%	5%	9%	13%	18%	23%	28%	33%	38%	42%	47%	50%	54%
Anchored-Brittle & H=9m-DS1	0%	4%	22%	42%	57%	67%	75%	81%	85%	88%	90%	92%	93%	95%	95%	96%
Anchored-Brittle & H=9m-DS2	0%	0%	3%	10%	21%	32%	42%	51%	58%	65%	70%	74%	78%	81%	83%	85%
Anchored-Brittle & H=9m-DS3	0%	0%	1%	3%	6%	10%	15%	21%	26%	32%	37%	42%	46%	50%	54%	58%
Anchored-Plastic & H=3m-DS1	0%	31%	57%	72%	81%	86%	90%	92%	94%	95%	96%	97%	97%	98%	98%	98%
Anchored-Plastic & H=3m-DS2	0%	7%	26%	45%	58%	68%	75%	80%	84%	87%	90%	91%	93%	94%	95%	96%
Anchored-Plastic & H=3m-DS3	0%	0%	0%	0%	0%	0%	0%	1%	1%	2%	2%	3%	4%	5%	6%	7%
Anchored-Plastic & H=4.5m-DS1	0%	8%	30%	49%	63%	72%	79%	83%	87%	89%	91%	93%	94%	95%	96%	96%
Anchored-Plastic & H=4.5m-DS2	0%	1%	12%	27%	41%	53%	62%	69%	75%	79%	83%	85%	88%	89%	91%	92%
Anchored-Plastic & H=4.5m-DS3	0%	0%	0%	0%	0%	0%	0%	1%	1%	1%	2%	3%	4%	5%	6%	7%
Anchored-Plastic & H=6m-DS1	0%	13%	38%	58%	70%	78%	84%	88%	91%	93%	94%	95%	96%	97%	97%	98%
Anchored-Plastic & H=6m-DS2	0%	3%	18%	36%	50%	62%	70%	77%	81%	85%	88%	90%	91%	93%	94%	95%
Anchored-Plastic & H=6m-DS3	0%	0%	0%	0%	0%	0%	0%	0%	1%	1%	2%	3%	4%	6%	7%	9%
Anchored-Plastic & H=7.5m-DS1	0%	11%	36%	55%	68%	77%	83%	87%	90%	92%	93%	95%	96%	96%	97%	97%
Anchored-Plastic & H=7.5m-DS2	0%	0%	5%	16%	28%	40%	50%	59%	65%	71%	75%	79%	82%	85%	87%	88%
Anchored-Plastic & H=7.5m-DS3	0%	0%	0%	0%	0%	1%	1%	2%	4%	6%	8%	11%	14%	17%	21%	24%
Anchored-Plastic & H=9m-DS1	0%	5%	25%	45%	60%	71%	78%	83%	87%	90%	92%	93%	94%	95%	96%	97%
Anchored-Plastic & H=9m-DS2	0%	0%	3%	12%	24%	36%	46%	55%	62%	68%	73%	77%	80%	83%	85%	87%
Anchored-Plastic & H=9m-DS3	0%	0%	0%	0%	1%	2%	4%	7%	11%	15%	20%	25%	29%	34%	39%	43%
Unanchored & H=3m-DS1	0%	14%	34%	49%	61%	69%	75%	79%	83%	86%	88%	90%	91%	92%	93%	94%
Unanchored & H=3m-DS2	0%	1%	8%	19%	30%	40%	49%	56%	62%	67%	72%	75%	78%	81%	83%	85%
Unanchored & H=3m-DS3	0%	0%	0%	1%	3%	5%	8%	12%	16%	20%	24%	28%	32%	36%	40%	43%
Unanchored & H=4.5m-DS1	0%	2%	13%	27%	39%	50%	59%	66%	71%	76%	79%	82%	85%	87%	88%	90%
Unanchored & H=4.5m-DS2	0%	0%	3%	10%	18%	28%	37%	45%	52%	58%	63%	67%	71%	74%	77%	80%
Unanchored & H=4.5m-DS3	0%	0%	0%	2%	4%	7%	11%	15%	20%	25%	29%	34%	38%	42%	46%	50%
Unanchored & H=6m-DS1	0%	5%	21%	38%	51%	62%	70%	76%	80%	84%	86%	89%	90%	92%	93%	94%
Unanchored & H=6m-DS2	0%	1%	6%	17%	29%	40%	50%	58%	64%	70%	74%	78%	81%	83%	85%	87%
Unanchored & H=6m-DS3	0%	0%	1%	2%	5%	9%	14%	18%	24%	29%	34%	38%	43%	47%	51%	55%
Unanchored & H=7.5m-DS1	0%	9%	31%	50%	64%	73%	79%	84%	87%	90%	92%	93%	94%	95%	96%	97%
Unanchored & H=7.5m-DS2	0%	0%	4%	12%	24%	35%	45%	53%	60%	66%	71%	75%	79%	81%	84%	86%
Unanchored & H=7.5m-DS3	0%	0%	1%	3%	6%	11%	16%	21%	27%	32%	38%	42%	47%	51%	55%	59%
Unanchored & H=9m-DS1	0%	4%	22%	41%	56%	67%	75%	81%	85%	88%	90%	92%	93%	94%	95%	96%
Unanchored & H=9m-DS2	0%	0%	3%	10%	21%	32%	42%	51%	58%	64%	69%	74%	77%	80%	83%	85%
Unanchored & H=9m-DS3	0%	0%	1%	3%	7%	13%	18%	24%	30%	36%	41%	46%	51%	55%	59%	62%

Table 12. Numerical values of probabilities of being in or exceeding a given *DS* for racking systems loaded with IBCs.

Drums:Anchored–Plastic: 3 m
Drums:Anchored–Brittle: 3 m
Drums:Unanchored: 3 m
Drums:Anchored–Plastic: 4.5 m
Drums:Anchored–Brittle: 4.5 m
Drums:Unanchored: 4.5 m
Drums:Anchored–Plastic: 6 m
Drums:Anchored–Brittle: 6 m
Drums:Unanchored: 6 m
Drums:Anchored–Plastic: 7.5 m
Drums:Anchored–Brittle: 7.5 m
Drums:Unanchored: 7.5 m
Drums:Anchored–Plastic: 9 m
Drums:Anchored–Brittle: 9 m
Drums:Unanchored: 9 m
DS1: nFF=1
DS2: nFF=2
DS3: nFF=3
DS1: nFF=2
DS2: nFF=3
DS3: nFF=4
DS1: nFF=2
DS2: nFF=3
DS3: nFF=5
DS1: nFF=2
DS2: nFF=4
DS3: nFF=6
DS1: nFF=3
DS2: nFF=5
DS3: nFF=7
P(DSI|PGA) [–]
PGA[g]
0
0.2
0.4
0.6
0.8
1
0.5
1.5

with

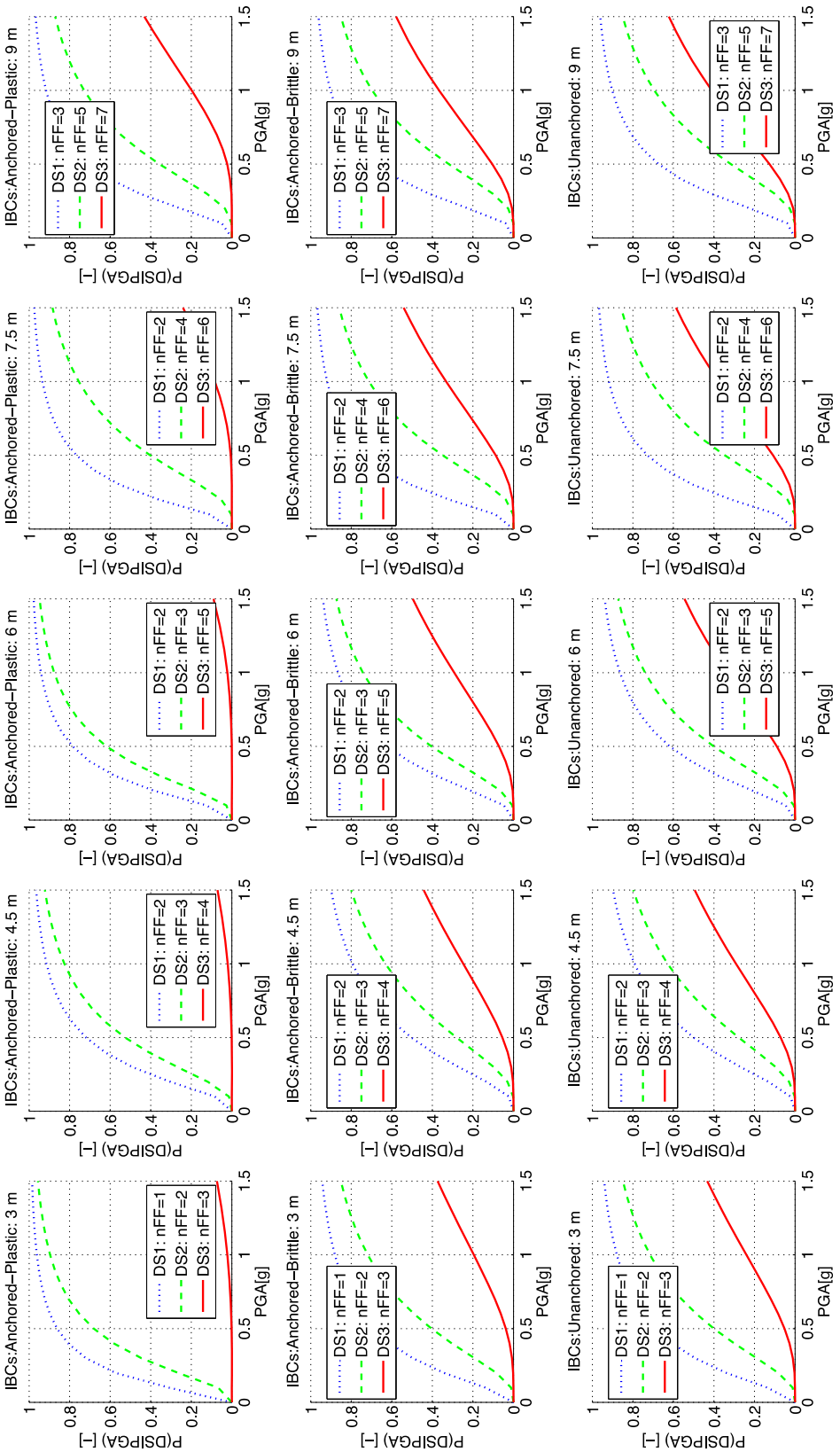
IBCs:Anchored–Plastic: 3 m
IBCs:Anchored–Plastic: 4.5 m
IBCs:Anchored–Plastic: 6 m
IBCs:Anchored–Plastic: 7.5 m
IBCs:Anchored–Plastic: 9 m
IBCs:Anchored–Brittle: 3 m
IBCs:Anchored–Brittle: 4.5 m
IBCs:Anchored–Brittle: 6 m
IBCs:Anchored–Brittle: 7.5 m
IBCs:Anchored–Brittle: 9 m
IBCs:Unanchored: 3 m
IBCs:Unanchored: 4.5 m
IBCs:Unanchored: 6 m
IBCs:Unanchored: 7.5 m
IBCs:Unanchored: 9 m
P(DSIPGA) [–]
PGA[g]
DS1: nFF=1
DS2: nFF=2
DS3: nFF=3
DS1: nFF=2
DS2: nFF=3
DS3: nFF=4
DS1: nFF=2
DS2: nFF=3
DS3: nFF=5
DS1: nFF=2
DS2: nFF=4
DS3: nFF=6
DS1: nFF=3
DS2: nFF=5
DS3: nFF=7

Fi s.

5 Case Study

This section provides a numerical example to assess the natech risk using the above fragility curves on chemical racks situated inside a warehouse. The RAPID-N (rapid natech risk assessment and mapping framework) was used to perform a simplified case study to assess the natech risk due to the 1786 Oliveri earthquake scenario. The framework assesses the risk of hazardous-material release, fire or explosion due to natural hazard impact (Girgin & Krausmann, 2013). This case study does not aim to assess the true risk level of the warehouse, but it aims to provide a demonstration of the potential impact of an earthquake on chemical racks. The 1786 Oliveri earthquake scenario was selected because it is well documented and a shake map calculated by the Instituto Nazionale di Geofisica e Vulcanologia (INGV) is available.

The Oliveri territory is located in one of the areas with the highest seismic potential of Sicily (Meletti and Valensise, 2004). The seismic activity recorded in the last 20 years is characterized by about 3500 events with local magnitude greater than 2 and hypocentres (89% of 3500) concentrated around an average depth of about 10 km (Giunta et al., 2004). Because of its high seismic hazard the urban area of Oliveri has been the subject of first level seismic micro-zonation. The first earthquake with a destructive effect in the Oliveri area, reported in the catalogue of historical Italian seismicity, occurred on 10 March 1786. This seismic event was characterized by M_w = 6.1, an epicentre with a depth of 10 km at Oliveri and an MCS intensity equal to IX in the urban area. This earthquake severely damaged all the cities of the Gulf of Patti in northern Sicily and almost destroyed the town of Oliveri (Guidoboni et al., 2007).

Since the industrial area of Milazzo is the closest industrial area to the epicentre of the 1786 Olivieri earthquake, eight types of chemical racks were assumed to be located inside a hypothetical chemical warehouse within the industrial area. Figure 10 shows the *PGA* distribution, provided by INGV for the 1786 earthquake that ranges from 0.01 to 0.4 g.

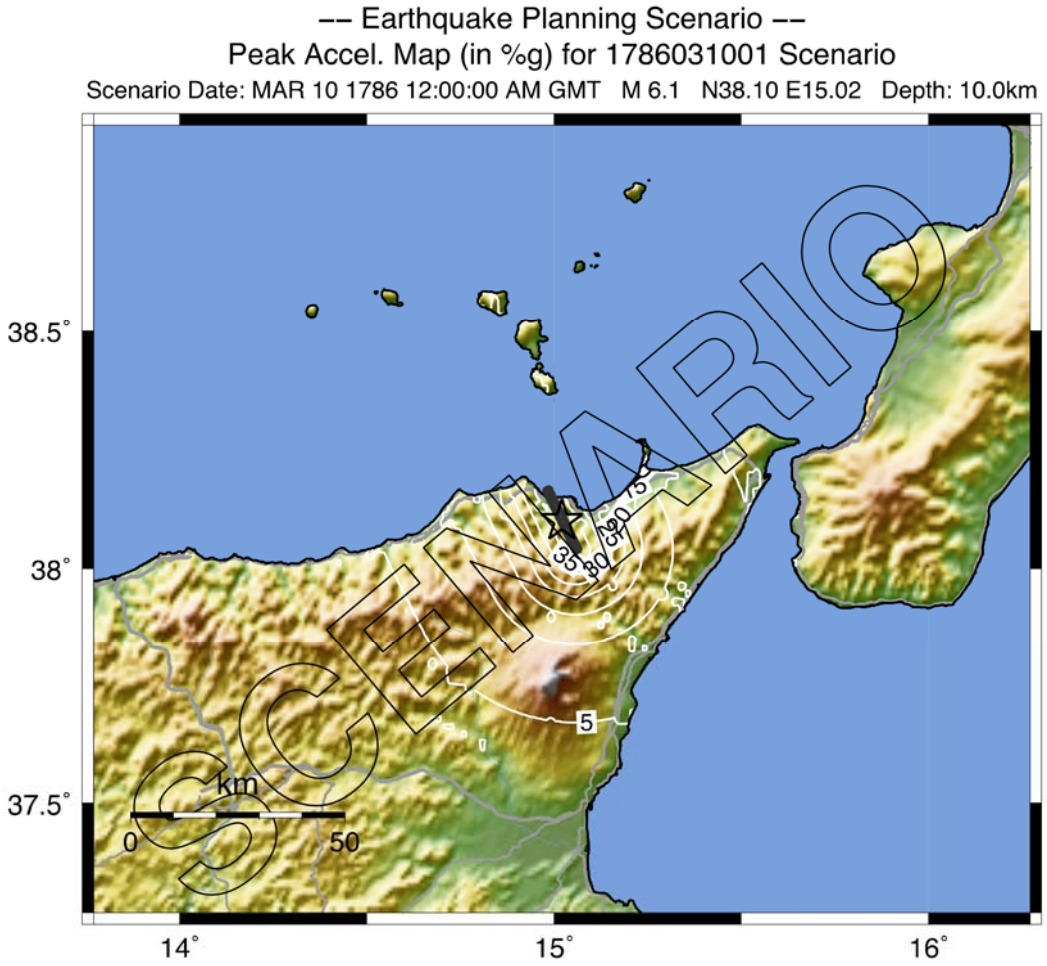

Figure 10. Distribution of on-site *PGA* for the 1786 Olivieri earthquake scenario (INGV, 2014).

In order to assess the natech risk of chemical racks containing a flammable substance, it is assumed that the chemical containers are filled with gasoline. The TNO Single Point model was used to calculate the end-point distances. The end-point radiation intensity was assumed to be 5003 W/m^2, which corresponds to 2nd degree burns (EPA, 1999). For liquid spills, the minimum pool depth that can be formed by the substance was assumed to be 1 cm as in the EPA methodology. Table 13 summarizes the characteristics of the chemical racks hypothesized for the case study.

Unit	Lenght [m]	Height [m]	Anchorage Type	Containers' Type	N° Containers	Substance	Filling Level	Q_{stored} [kg]
R01	9	3	Unanchored	IBC	24	Gasoline	80%	14208
R02	9	4.5	Unanchored	IBC	32	Gasoline	80%	18944
R03	9	4.5	Anchored-Brittle	IBC	32	Gasoline	80%	18944
R04	9	9	Anchored-Plastic	IBC	56	Gasoline	80%	33152
R05	9	3	Unanchored	Drum	24	Gasoline	80%	11366
R06	9	4.5	Unanchored	Drum	32	Gasoline	80%	15155
R07	9	4.5	Anchored-Brittle	Drum	32	Gasoline	80%	15155
R08	9	9	Anchored-Plastic	Drum	56	Gasoline	80%	26522

Table 13. Characteristics of the chemical racks.

Based on the input information of chemical racks discussed above and the ShakeMap provided by INGV for the 1786 Olivieri earthquake scenario, the results of the case study– as provided as RAPID-N outputs – are shown in Table 14. RAPID-N automatically determined that the industrial site is about 25 km away from the epicentre and that it was subjected to an on-site *PGA* of about 0.11 g. Depending on rack type and the on-site hazard parameters, RAPID-N selects the appropriate fragility curve and estimates the damage states and the consequence scenarios. In this case study, the released substance quantity (i.e., the so called $Q_{Released}$) is assumed to be the same as the percentage of containers that fall from the racking system.

		DS0		*DS1*				*DS2*				*DS3*			
Unit	*PGA*	P_{DS}	$Q_{Released}$	P_{DS}	$Q_{Released}$	d_{EP}	P_N	P_{DS}	$Q_{Released}$	d_{EP}	P_N	P_{DS}	$Q_{Released}$	d_{EP}	P_N
	[m/s^2]	[-]	[kg]	[-]	[kg]	[m]	[-]	[-]	[kg]	[m]	[-]	[-]	[kg]	[m]	[-]
R01	1.068	84.5%	0	13.98%	4689	119	2.80%	1.50%	9519	170	0.30%	0.01%	14208	207	0.003%
R02	1.068	97.1%	0	2.66%	9472	169	0.53%	0.23%	14208	207	0.05%	0.02%	18944	239	0.005%
R03	1.068	97.0%	0	2.71%	9472	169	0.54%	0.24%	14208	207	0.05%	0.01%	18944	239	0.003%
R04	1.068	93.6%	0	6.17%	16576	224	1.23%	0.19%	24864	274	0.04%	0.00%	-	-	-
R05	1.068	99.6%	0	0.39%	5683	131	0.08%	0.00%	-	-	-	0.01%	11366	185	0.002%
R06	1.068	100.0%	0	0.00%	-	-	-	0.00%	-	-	-	0.02%	15155	214	0.005%
R07	1.068	100.0%	0	0.00%	-	-	-	0.00%	-	-	-	0.01%	15155	214	0.003%
R08	1.068	100.0%	0	0.00%	-	-	-	0.00%	-	-	-	0.00%	-	-	-

P_{DS} = Probability to be in a certain DS; P_N = Natech Probability related to a DS; d_{EP} = Pool fire's end-point distance

Table 14. Summary of the natech risk assessment results for chemical racks.

According to the results of this RAPID-N test case, the minimum end-point distance for receiving 2nd degree burns is found to be 119 m with an occurrence probability of 2.8%, whereas the maximum is 239 m with a probability of 0.005%. Potential domino effects should also be considered for a more accurate assessment of the natech risk. The current version of RAPID-N does not yet support these features.

Moreover, the results indicate that possibly major natech accidents are to be expected in chemical racks loaded with IBCs, because they have a lower friction coefficient and a higher weight. Although the racks R02 and R03 have the same load and height, the falling probabilities *DS1* and *DS2* of R03 are higher than those of R02, because the robustness of the anchorage increases the PFA intensity.

6 Conclusions

This work presented an approach for developing fragility curves for chemical racking systems in the cross-aisle direction through dynamic non-linear analyses. The damage state limits of the

overall racking system were defined as four levels of intensity of loss of rack containment, i.e. the percentage of containers that fall from the steel storage rack. These are: *DS0* = no losses, *DS1* = moderate losses (≥30% of falls), *DS2* = extensive losses (≥60% of falls), and *DS3* = complete losses of containment (100% of falls). In order to evaluate the structural vulnerability of the chemical containers and of the overall racking system, three damage modes (i.e., overturning, sliding, and buckling) were identified. Analytical fragility curves – as a function of the *PFA* – were constructed for each damage mode. A fault tree model was used to evaluate the falling probabilities of chemical containers from racks as a function of the *PGA* combining the fragility curves of the three damage modes. In order to assess the seismic vulnerability of a suite of chemical racking systems that respect the height limits for fire protection, to evaluate the effect of the anchorage on the seismic performance, and to study the influence of the friction coefficient between chemical containers and the rack's beams, two types of chemical containers (205 l metal drums and 1000 l IBCs), three types of rack base anchoring (unanchored, anchored-brittle, and anchored-plastic), and four rack heights (3, 4.5, 6, 7.5, 9 m) were studied. Overall twenty-four fragility curves were developed. As an input motion to the three damage models, twenty-six strong motion records were selected from the PEER Strong Motion database.

In order to assess the natech risk of a chemical rack containing a flammable substance, to test the developed fragility curves, and to illustrate the natech risk assessment and mapping capabilities of RAPID-N, a case study based on the 1786 Olivieri earthquake scenario was conducted. The findings demonstrate that chemical racks loaded with IBCs are more vulnerable than those loaded with drums, because they have a lower friction coefficient and a higher weight. Moreover, although a robust anchorage reduces the probability of collapse of the rack, it increases the *PFA* intensity and therefore the probabilities of falling *DS1* and *DS2*.

Further studies using different layouts and types of merchandise chemical containers and of storage racks representing current construction practices and innovative systems are necessary to refine the fragility curve development for chemical racking structures. Moreover, the rack behaviour in the down-aisle direction and the structural interaction between neighbouring racks were not considered for constructing the analytical fragility curves in this study. Inclusion of these aspects in future studies is necessary. However, the analytical method employed in this study can be used for deriving fragility curves for others merchandise types of racking structures.

7 Bibliography

ADR (2012). Applicable as from 1 January 2013: European Agreement Concerning the International Carriage of Dangerous Goods by Road. New York: United Nations.

ANSI (1997). American National Standard for Steel Drums and Pails, *ANSI MH2-1997: American National Standards Institution.*

A.S. 4084 (1993). Steel Storage Racking, *Australian Standards*.

Agresti, A. (2012). *Categorical data analysis*. Wiley, New York.

Bajoria, K. M. (1986). *Three dimensional progressive collapse of warehouse racking* (Doctoral dissertation, University of Cambridge).

Baldassino, N., & Zandonini, R. (2001). Numerical and Experimental Analysis of Base-plate Connections of Steel Storage Pallet Racks. *Proc. of XVIII Conference C.T.A.*, (pp. 127-136). Venezia.

Blume, J. A. & Associates (1973). Seismic Investigation of Steel Industrial Storage Racks. Rack Manufacturer's Institute, San Francisco, CA.

Boca, G., Ozunu, A., & Vlad, Ş. (2010). Natech Risk And Management: An Assessment Of The Tarnavelor Plateau's Specific Hazards. *Present Environment And Sustainable Development, 4*, 269-276.

Calvi, G. (1999). A displacement based approach for vulnerability evaluation of classes of buildings. *Earthquake Eng, 3* (3), 411–38.

Castiglioni, C. (2008). Seismic behaviour of steel storage pallet racking systems. Milano: Politecnico di Milano – Dipartimento di Ingegneria Strutturale.

Chen, C., Scholl, R., & Blume, J. (1980a). Seismic Study of Industrial Storage Racks. National Science Foundation and for the Rack Manufacturers Institute and Automated Storage and Retrieval Systems (sections of the Material Handling Institute). San Francisco, CA: John A. Blume & Associates.

Chen, C., Scholl, R., & Blume, J. (1980b). Earthquake Simulation Tests of Industrial Steel Storage Racks. *Seventh World Conference on Earthquake Engineering*, (pp. 379-386). Istanbul, Turkey.

Chen, C., Scholl, R., & Blume, J. (1981). Seismic-Resistant Design of Industrial Storage Racks. *Second Specialty Conference on Dynamic Response of Structures: Experimentation, Observation and Control*, (pp. 745-759). Atlanta, GA .

Chopra, A. K. (1995). Dynamics of structures: Theory and applications to earthquake engineering. Englewood Cliffs, N.J: Prentice Hall.

Crowley, H., Pinho, R., & Bommer, J. (2004). A probabilistic displacement-based vulnerability assessment procedure for earthquake loss estimation. *Bull. Earthquake Eng., 2*, 173–219.

D'Hollander, O.J.L. (1993). U.S. Patent No. 5,269,414. *Washington, DC: U.S. Patent and Trademark Office.*

Di Stefano, P., Luzio, D., Renda, P., Martorana, R., Capizzi, P., D'Alessandro, A., & Zarcone, G. (2014). Integration of HVSR measures and stratigraphic constraints for seismic microzonation studies: the case of Oliveri (ME). *Nat. Hazards Earth Syst. Sci. Discuss.*, 2(4), 2597–2637. doi:10.5194/nhessd-2-2597-2014.

Denoël, V., & Degée, H. (2005). *Cas particulier d'étude analytique de l'élément à frottement.* Internal report 2005-1, University of Liege, Department M&S.

EPA (1999). Risk Management Program Guidance for Offsite Consequence Analysis.

Eurocode 3, Design of steel structures, ENV 1993.

FEM 10.2.02 (2001). The Design of Static Steel Pallet Racks, Federation Europeen de la Manutention, Vers. 1.02.

FEM 10.2.08 (2005). The Seismic Design of Static Steel Pallet Racks, Federation Europeen de la Manutention, final draft, December 2005.

FEMA (1999). *HAZUS earthquakes loss estimation methodology.* Washington: US Federal Emergency Management Agency.

FEMA (2012). *Seismic Performance Assessment of Buildings (FEMA P-58).* Washington, D.C.: ATC-58, Applied Technology Council.

Filiatrault, A., & Wanitkorkul, A. (2004). *Shake Table Testing of Frazier Industrial Storage Pallet Racks.* Report No. CSEE-SEESL-2004-02, University at Buffalo, State University of New York, Buffalo, NY.

Girgin, S. (2011). The natech events during the 17 August 1999 Kocaeli earthquake: aftermath and lessons learned. *Natural Hazards and Earth System Sciences, 11*, 1129–1140.

Girgin, S., & Krausmann, E. (2013). RAPID-N: Rapid natech risk assessment and mapping framework. *Journal of Loss Prevention in the Process Industries*, 26(6), 949–960. doi:10.1016/j.jlp.2013.10.004; http://rapidn.jrc.ec.europa.eu

Giunta, G., Luzio, D., Tondi, E., De Luca, L., Giorgianni, A., D'Anna, G., Renda, P., Cello, G., Nigro, F., & Vitale, M. (2004). The Palermo (Sicily) seismic cluster of September 2002, in the seismotectonic framework of the Tyrrhenian Sea-Sicily border area, *Ann. Geophys.-Italy*, 47, 1755–1770.

Guidoboni, E., Ferrari, G., Mariotti, D., Comastri, A., Tarabusi, G., & Valensise, G. (2007). Catalogue of Strong Earthquakes in Italy (CFTI), 461BC–1997 and Mediterranean Area 760BC–1500, available at: http://storing.ingv.it/cfti4med/.

Housner, G. W. (1963). *The behaviour of inverted pendulum structures during earthquakes*. Bull. Seismological Soc. of America 53: 404-17.

HSE (2009). *Chemical warehousing-The storage of packaged dangerous substances.* Sudbury, Suffolk: HSE Books.

HSE (2007). Warehousing and storage: a guide to health and safety. Sudbury, Suffolk: HSE Books.

INGV (2014). Earthquake Planning Scenarios. Retrieved October 21, 2014, from http://shakemap.rm.ingv.it/shake/archive/scenario.html

Krausmann, E., Cozzani, V., Salzano, E., Renni, E. (2011). Industrial accidents triggered by natural hazards: an emerging risk issue, *Natural Hazards and Earth System Sciences*, 11(3), 921-929.

Krausmann, E., & Cruz, A. (2013). Impact of the 11 March 2011, Great East Japan earthquake and tsunami on the chemical industry. *Natural Hazards, 67*, 811–828.

Krausmann, E., Cruz, A., & Affeltranger, B. (2010). The impact of the 12 May 2008 Wenchuan earthquake on industrial facilities. *Journal of Loss Prevention in the Process Industries, 23* (2), 242–248.

Krawinkler, H., Cofie, N., Astiz, M., & Kircher, C. (1979). *Experimental Study on the Seismic Behavior of Industrial Storage Racks.* The John A. Blume Earthquake Engineering Center, Department of Civil Engineering. Stanford, CA: Stanford University.

Makris, N., & Zhang, J. (1999). *Rocking Response and Overturning of Anchored Equipment under Seismic Excitations.* PEER Report 1999/06, Pacific Earthquake Engineering Research Center, University of California, Berkeley, California.

Meletti, C., & Valensise, G. (2004). Zonazione sismo genetica ZS9 – A 2 pp. al Rapporto Conclusivo, available at: http://zonesismiche.mi.ingv.it/documenti/A2pp.pdf.

Ng, A. L. Y., Beale, R. G., & Godley, M. H. R. (2009). Methods of restraining progressive collapse in rack structures. *Engineering Structures*, *31*(7), 1460-1468.

NWPCA (1996). Uniform standard for wood pallets. Arlington, VA: National Wooden Pallet and Container Association.

OFC (2006). 2007 Oregon fire code. County Club Hills, Il. International Code Council Beaverton, OR: distributed by Building Tech Bookstore.

Pinto, P., Giannini, R., & Franchin, P. (2004). *Methods for seismic reliability analysis of structures.* Pavia, Italy: IUSS Press.

RAL (1990). Storage and Associated Equipment, Deutsches Institut für Gutersichcherung und Kennzeichnung (German Institute for Quality Assurance and Marketing).

RMI (2002a). Specification for the design testing and utilization of industrial steel storage racks, Rack Manufacturers Institute, Charlotte, NC. 2002 edition.

RMI (2002b). Commentary to Specification for the design testing and utilization of industrial steel storage racks, Rack Manufacturers Institute, Charlotte NC.

Sasani, M., Der Kiureghian, A., & Bertero, V. (2002). Seismic fragility of short period reinforced concrete structural walls under near-source ground motions. *Structural Safety* .

Shenton, H. W. (1996). Criteria for initiation of slide, rock, and slide-rock rigid-body modes. *J. of Engrg. Mech. Div., 122*, 690-693.

Showalter, P.S., & Myers, M.F. (1994). Natural disasters in the United States as release agents of oil, chemicals, or radiological materials between 1980-9: analysis and recommendations, *Risk Analysis,* 14(2), 169-181.

Singhal, A., & Kiremidjian, A. (1996). Method for probabilistic evaluation of seismic structural damage. *Journal of Structural Engineering, 122*, 1459–1467.

Tugnoli, A., Cozzani, V., & Landucci G. (2007). A consequence-based approach to the quantitative assessment of inherent safety, AIChE J. 53, 3171-3182.

8 List of symbols

PGA	Peak ground acceleration;
$MI_{i,j}$	Motion intensity at the ith rack's floor for the jth damage mode;
μ_j	Mean of the lognormal distribution for the jth damage mode;
σ_j	Standard deviation of the lognormal distribution for the jth damage mode;
DS	Damage state;
$P_j[DS\|MI_{i,j}]$	Probability for a jth damage mode that a certain damage state is exceeded, given a specific value of motion intensity at the ith rack's floor;
Φ	Lognormal cumulative distribution function;
$P[DS\|PGA]$	Probability of being in or exceeding a given DS, i.e. the vulnerability of racking system to lose its containment;
n_{FF}	Number of simultaneous "floor's failures" – i.e., when all containers of a given floor fall – needed to have the loss intensity defined by a given DS;
X_j	Parameters that describe the failure of the system for each jth damage mode (i.e., the system fall if $X_j \geq 1$);
$P_{l,i}$	Falling probability of containers from the ith floor;
$P_{L,k}$	Vector sorted in descending order of the floor's failures probabilities $P_{l,i}$;
H	Height;
Δh_F	Inter-floor height;
Y_{DS}	Percentage that describes the loss intensity of rack containment (i.e., limit percentage of containers that fall from the frame: $DS0$=0%, $DS1$=30%, $DS2$=60%, and $DS3$=100%);
PFA_i	Median peak floor acceleration
$a_{cr,j}$	"Critical horizontal accelerations" related to the jth failure mechanism;
h_i	Height of the ith floor;
a_k	Regression coefficients of the polynomial prediction equation to determinate the PFA_i is the median Peak Floor Acceleration
ϑ	Rotation that describe the motion of the rigid block;
I_0	Moment of inertia about pivot point O or O';
m	Mass of the block;
R	Distance between the centre of gravity and the centre of rotation;
g	Gravity acceleration;
α	Angle defined in Figure 5;
$\ddot{u}_g$	Ground acceleration;
K_{el}	Elastic stiffness of the anchorage;
$f(\vartheta)$	A function that models the nonlinear hysteretic behaviour of the anchorage;
$\dot{\vartheta}_{\text{after impact}}$	Rotational velocity after the impact;
$\dot{\vartheta}_{\text{before impact}}$	Rotational velocity before the impact;

η	Restitution coefficient;
p	Frequency parameter of the rigid block;
K_{pl}	Plastic stiffness of the anchorage;
F_Y	Yielding load of the anchoring;
F_U	Ultimate load of the anchoring;
ϑ_Y	Elastic range rotation;
ϑ_U	Ultimate rotation;
$H()$	Heaviside function;
ϑ_χ	A variable that changes on each integration step (see Figure 6);
ϑ_χ^-	Value of the variable before the integration step;
ϑ_χ^+	Value of the variable after the integration step;
$a_{st,j}$	Static horizontal acceleration needed to break the anchorage;
ϑ_{c}	"Critical rotation" that maximise the value of $a_{st,j}$;
$F_{cr}(\vartheta_{c})$	"Equivalent anchorage strength";
α_{eq}	Equivalent angle α;
R_{eq}	Equivalent distance between the centre of gravity and the centre of rotation;
μ_S	Static friction coefficient;
μ_d	Dynamic friction coefficient;
u	Mass displacement;
Δu	Relative displacement between the mass and the support;
Δv	Relative velocity between the mass and the support;
Δu_{Lim}	Relative displacement limit
m_i	Floor's masses;
$\{u\}$	Vector of floor horizontal displacements;
$[C]$	Damping matrix;
$[K_S]$	Stiffness matrix of the racking system considering the shear flexibility;
$[K_S]$	Stiffness matrix of the racking system considering the bending flexibility;
I	Inertia of the cantilever beam;
b	Inter-column distance in the cross-aisle direction;
A_C	Area of the upright columns;
I_C	Inertia of the upright columns;
A_B	Area of the bracing trusses;
E_B	Elastic modulus of the bracing trusses;
φ	Angle defined in Figure 3a;
k_S	Floor bracing stiffness;
N_{MAX}	Maximum axial load due to the seismic ground motion acting on the diagonal bracing truss of the first floor;
N_{cr}	Critical buckling load – assuming a buckling length factor equal to 0.5 – acting on the diagonal bracing truss of the first floor;

I_B	Inertia of the diagonal truss;
$F_{1,MAX}$	Maximum absolute elastic force at the first floor;
Δh_B	"Span" of the bracing system assuming a K-form;
Q_{Stored}	Substance stored;
$Q_{Released}$	Substance released;
P_{DS}	Probability to be in a certain DS;
P_N	Natech Probability related to a DS;
d_{EP}	Pool fire's end-point distance.

European Commission
EUR 26953 EN – Joint Research Centre – Institute for the Protection and Security of the Citizen

Title: Seismic Vulnerability of Chemical Racks in the Cross-Aisle Direction

Authors: Vincenzo Arcidiacono, Serkan Girgin, Elisabeth Krausmann

Luxembourg: Publications Office of the European Union

2014 – 33 pp. – 21.0 x 29.7 cm

EUR – Scientific and Technical Research series – ISSN 1831-9424

ISBN 978-92-79-44410-4

doi:10.2788/65727

LB-NA-26953-EN-N

JRC Mission

As the Commission's in-house science service, the Joint Research Centre's mission is to provide EU policies with independent, evidence-based scientific and technical support throughout the whole policy cycle.

Working in close cooperation with policy Directorates-General, the JRC addresses key societal challenges while stimulating innovation through developing new methods, tools and standards, and sharing its know-how with the Member States, the scientific community and international partners.

Serving society
Stimulating innovation
Supporting legislation

doi:10.2788/65727

ISBN 978-92-79-44410-4

Publications Office